NTIA Report TR-12-484

Free-Field Measurements of the Electrical Properties of Soil Using the Surface Wave Propagation Between Two Monopole Antennas

January 2012

report series

U.S. DEPARTMENT OF COMMERCE • National Telecommunications and Information Administration

NTIA Report TR-12-484

Free-Field Measurements of the Electrical Properties of Soil Using the Surface Wave Propagation Between Two Monopole Antennas

Nicholas DeMinco
Robert T. Johnk
Paul McKenna
Chriss A. Hammerschmidt
J. Wayde Allen

U.S. DEPARTMENT OF COMMERCE

December 2011

DISCLAIMER

Certain commercial equipment and materials are identified in this report to specify adequately the technical aspects of the reported results. In no case does such identification imply recommendations or endorsement by the National Telecommunications and Information Administration, nor does it imply that the material or equipment identified is the best available for this purpose.

CONTENTS

Page

FIGURES

TABLES

Page

FREE-FIELD MEASUREMENTS OF THE ELECTRICAL PROPERTIES OF SOIL USING THE SURFACE WAVE PROPAGATION BETWEEN TWO MONOPOLE ANTENNAS

Nicholas DeMinco, Robert T. Johnk, Paul McKenna,
Chriss A. Hammerschmidt, J. Wayde Allen[1]

This report describes one of three free-field radio frequency (RF) measurement systems that are currently being developed by engineers at the Institute for Telecommunication Sciences (NTIA/ITS). The objective is to provide estimates of the electrical properties of the ground (permittivity and conductivity) over which the measurement systems are deployed. This measurement system uses transmission loss measurements between two monopoles placed close to the ground at specific separation distances. Soil properties are extracted by comparing measured data with known analytical models and optimizing the results.

Key words: antenna; radio-wave propagation; deconvolution; Fourier transform; frequency domain; gating; monopole antenna; reflectivity, signal processing, S-parameters, time domain; transmission loss; propagation measurement

1 INTRODUCTION

A near-earth propagation measurements program was initiated at the Institute for Telecommunication Sciences (NTIA/ITS) Table Mountain Field Site (TMFS) in August 2009 under the sponsorship of the Naval Research Laboratory (NRL). A second set of measurements sponsored by the Table Mountain Research Project were performed in May 2010. The purpose of these efforts was to develop improved propagation prediction tools and models for close-in distances (2–250 m) and low antenna heights (0–3 m). While comparing measured and modeled results, questions arose about the assumed dielectric permittivity and conductivity of the soil at the TMFS. These ground constants can have a significant influence on RF propagation predictions near the ground and need to be accurately characterized.

The system described in Section 2 of this report performs two-port transmission measurements between two resonant ground-plane mounted monopoles placed at various separation distances ranging from 2 to 250 meters. The measurements were conducted along a main access road at various road positions using stepped-frequency transmission measurements over the Earth between the monopoles. For the set of measurements taken in August 2009, the separation distances were varied within the full range; for the second set of measurements taken in May 2010, the separation distance was fixed at 8.3 meters. It is desirable to locate the antennas as close to ground as possible, so that the predominant mode of propagation is by means of the surface wave. The monopoles were placed 8.9 centimeters above ground to simplify feeding the

[1] The authors are with the Institute for Telecommunication Sciences, National Telecommunications and Information Administration, U.S. Department of Commerce, Boulder, CO 80305.

antenna from below the ground plane while maintaining the antenna height as close to zero with respect to a wavelength as possible.

For the frequencies under consideration (30 to 915 MHz), this is essentially equivalent to a zero height antenna, because the wavelengths are between 0.328 and 10.0 meters. The propagation between the antennas is predominantly via the Norton surface wave [1]–[3], because the antennas are very close to the Earth. At this height, the direct and reflected waves cancel each other, resulting in only the surface wave component of the ground wave as the mechanism for radio-wave propagation. The skin depth of the propagating wave into the soil is significant, so the use of the surface wave effectively probes the ground, resulting in an aggregate measure of the ground constants of the soil. Actual skin depths for different values of sigma (σ) and epsilon (ε_r) will be presented in Section 4.

2 MONOPOLE TRANSMISSION MEASUREMENT SYSTEM

The system, a schematic of which is shown in Figure 1, uses a vector network analyzer (VNA) to perform stepped-frequency transmission (S-parameter) measurements over a wide frequency range between two resonant monopoles separated at a distance *d*. The monopoles are mounted at the center of circular aluminum ground planes, and are coaxially fed on the bottom side of the ground planes. Each antenna is soldered to a coaxial feedthrough that provides a type-N connection from the bottom. Dielectric spacers on the plates provide enough clearance for a coaxial cable to feed the monopoles.

The nominal height of the ground planes is h_1=h_2=8.9 cm. The VNA is configured to perform stepped-frequency measurements of the S-parameter S_{21}. Measurement data were acquired over a frequency range from 300 kHz to 6 GHz. Data for the analysis was extracted from this measurement set over a frequency range subset of 30 MHz to 915 MHz, because of the limited dynamic range outside the operating frequency range of the resonant monopole antennas.

The system is calibrated by connecting the transmitting and receiving cables together and performing a through calibration. The cables are then connected to the antennas and the transmission loss is measured.

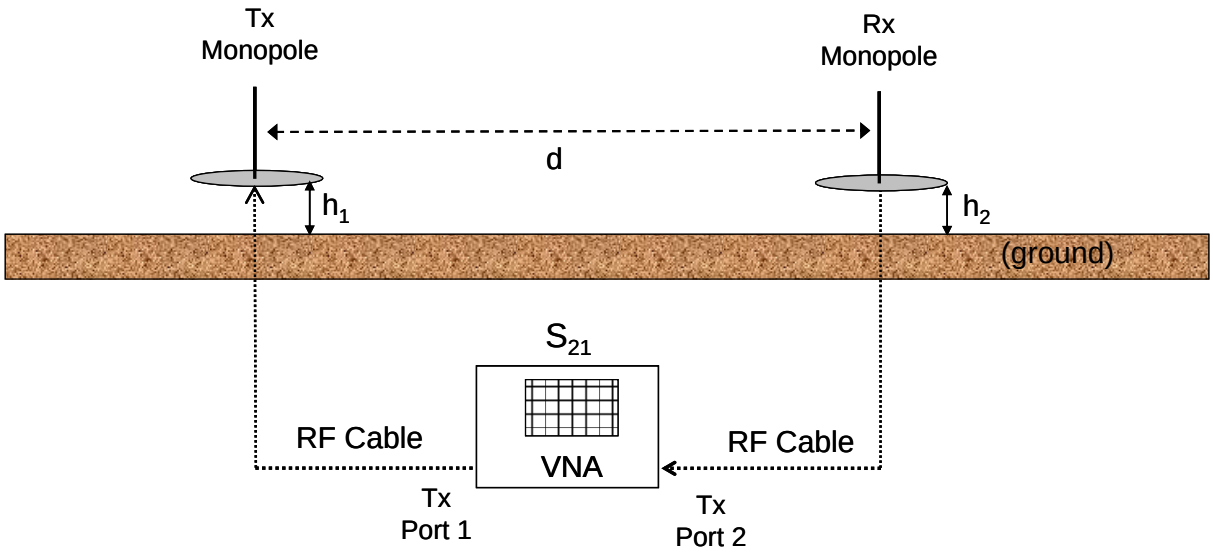

Figure 1. Schematic diagram of the monopole measurement system.

Both magnitude and phase information are acquired, which permits transformations to and from the time and frequency domain. This capability provides more insight into the propagation over the ground and permits processing to enhance accuracy and signal fidelity by windowing the stepped frequency data and time gating the time domain waveform.

A flow chart showing the signal processing sequence is shown in Figure 2. These stepped-frequency data are windowed to suppress undesired out-of-band effects, then inverse Fourier transformed to obtain a time-domain waveform. Time gating is then applied to isolate the desired propagation events and to improve signal-to-noise performance. Finally, the gated waveform is

Fourier transformed to yield the gated S_{21g}. Figure 3 depicts the results of this process and shows the influence on the amplitude spectra when the effects of a nearby reflector are removed using time gating. The corresponding ungated and gated time domain waveforms are shown in Figure 3(b). The presence of a nearby scatterer manifests itself in the secondary wavelet that follows the main propagation event. After this packet is gated out and Fourier transformed, the resulting S_{21} is smoothed out and systematic scalloping is removed. A combination of signal processing and time gating were used to remove the effects of nearby reflectors and scatters to isolate the coupling between the antennas. This produces a significant improvement in signal fidelity and signal-to-noise ratio.

The surface wave loss measurements at the TMFS were performed by measuring the propagation loss between two matched monopole antennas each mounted on a separate circular ground planes using techniques described in the previous paragraphs. The ground constants are determined by using the measured loss of the surface wave between two antennas at known distances. The antennas were a set of quarter-wave monopoles resonant at 150, 250, 430, 700, and 915 MHz. The ground planes were approximately one-quarter wavelength in radius. The antennas were spaced at known separation distances and placed on the ground at a height of approximately zero meters (8.9 cm) above ground. Practical limitations of feeding the antennas prevented heights less than 8.9 cm, but analysis has verified that there is a negligible difference in results between the 8.9 cm and zero antenna heights.

The approach was to compute the propagation losses between the two antennas at the fixed distances for a variety of ground constants and frequencies and match the measured losses to the appropriate curves to obtain the various ground constants. The distances between the antennas at which measurements were taken in 2009 included: 2, 3, 4, 5, 8, 10, 15, 20, 25, 30, 35, 40, 50, 80, 100, 150, 180, 200, and 250 meters. Data for this scenario reflects a road section with a flat terrain measurement environment. The portion of the path used for performing the measurements was line-of-sight. The frequency was stepped from 300 kHz to 6000 MHz while the antennas remained stationary at each of the distances listed above. In 2010, a second set of measurement data was taken at the same location, but only at a fixed distance of 8.3 meters.

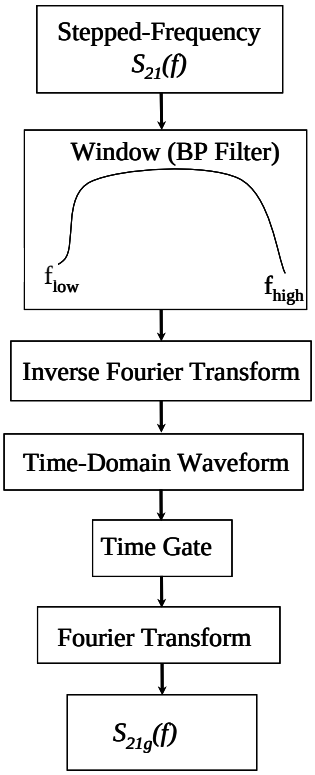

Figure 2. Flowchart of the sequence used to post process the monopole transmission measurements.

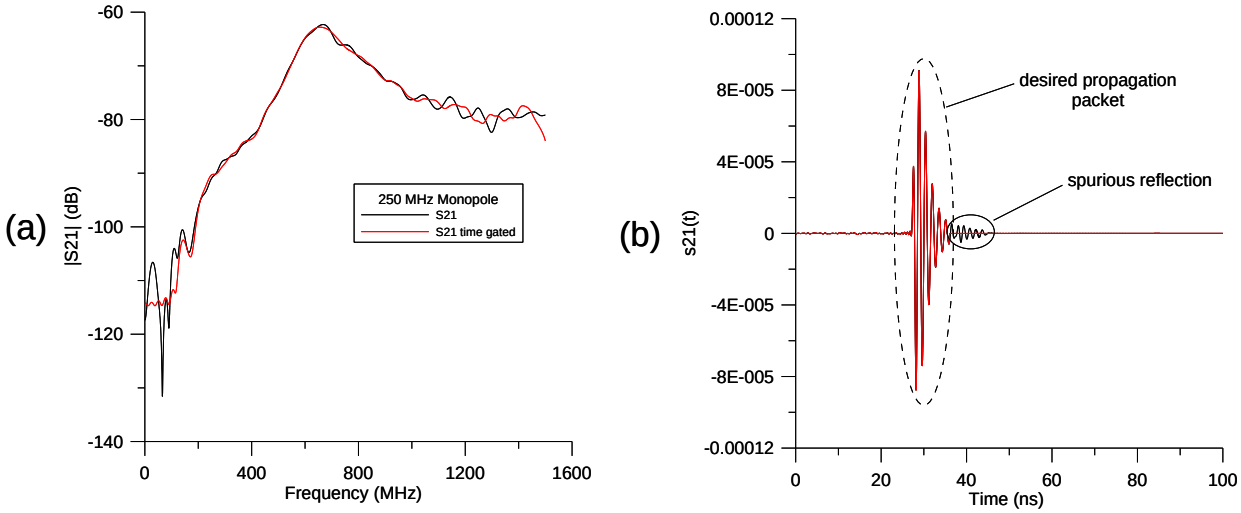

Figure 3. (a) Ungated and time-gated (0–36 ns) amplitude spectra for 700 MHz resonant monopoles separated at d = 8 m. (b) Corresponding gated and ungated time-domain waveforms.

3 GROUND-WAVE PROPAGATION COMPUTATION METHOD AND THE DEVELOPMENT OF THE UNDISTURBED-FIELD MODEL

The ground wave includes the direct line-of-sight space wave, the ground-reflected wave, and the Norton surface wave that propagates along the Earth. The Norton surface wave will hereafter be referred to as a surface wave in this report. Propagation of the ground wave depends on the relative geometry of the transmitter and receiver locations and antenna heights. The radio wave propagates primarily as a surface wave when both the transmitter and receiver antennas are close to the Earth (approximately 0.25 wavelength or less), because the direct and ground-reflected waves in the space wave components of the ground wave cancel each other out. As a result, the surface wave is the only wave component that continues to propagate.

This cancellation occurs because the elevation angle is zero, the two waves (direct and reflected) are equal amplitude and opposite in phase, and they travel the same distance. The surface wave is predominantly vertically polarized, since the ground conductivity effectively attenuates most of the horizontal electric field component at a rate many times that for the vertical component of the electric field. When one or both antennas are elevated above the ground to a significant height with respect to a wavelength (greater than 0.25 wavelength), the space wave predominates.

When the antennas are close to the ground with respect to a wavelength, the surface wave propagates along and is guided by the Earth's surface. This is similar to the way that an electromagnetic wave is guided along a transmission line. The attenuation of this wave is directly affected by the ground constants of the Earth along which it travels [1]. Charges induced in the Earth by the surface wave travel with the surface wave and create a current in the Earth. The Earth carrying this current can be modeled as a leaky capacitor (a capacitive reactance shunted by a resistance). The characteristics of the Earth as a conductor are therefore represented by this equivalent parallel resistor-capacitor circuit. The Earth's conductivity acts as a resistor and the Earth's dielectric constant acts as a capacitor. As the surface wave passes over the surface of the Earth, it is attenuated due to the current flowing through the Earth's resistance. Energy is taken from the surface wave to supply the losses in the ground.

Since the equivalent circuit of the Earth is a resistor of resistance R (ohms) and capacitor of capacitance C (Farads) in parallel, more current flows through the resistance at lower frequencies, $R << 1/\omega C$ ($\omega = 2\pi f$ where f is the frequency in Hertz); and the attenuation factor is then primarily dependent on the conductivity of the Earth and the frequency. At lower HF frequencies, AM broadcast (medium frequencies), and lower frequencies in the LF band (below 300 kHz), the Earth can be regarded as being purely resistive in nature. For frequencies above about 150 MHz, the impedance represented by the Earth is primarily capacitive, so the attenuation factor for the surface wave at a given physical distance is determined by the dielectric constant of the Earth and the frequency [1]. The impedance of the capacitor decreases with increasing frequency.

The ITS Undisturbed-Field Model was originally developed for very short-range propagation for distances of 2 to 30 meters. Subsequently, the model was shown to be accurate for flat terrain up to 2 kilometers [2]. The minimum distance is based on staying at distances greater than the distance within which the reactive field of the antenna is present. This is a distance of one wavelength. Extensive testing with exact models at close-in distances has verified the

computation accuracy for distances as close as 2 meters over the 150 MHz to 6000 MHz frequency band [2].

This method involves the calculation of the undisturbed electric field as a function of antenna heights, distance, frequency, and the ground constants from which the path loss is derived. The undisturbed field is that electric field produced by a transmitting antenna at different distances and heights above ground without any field-disturbing factors such as other receiver antennas in the proximity of the receiver antenna location. The undisturbed electric field technique includes near-field effects of the transmit antenna, the complex two-ray model, antenna near-field and far-field response, and the surface wave. Since this is a line-of-sight model, the ground is assumed to be flat over the distance of 2 kilometers or less with no irregular terrain present. For distances of less than 5 kilometers, the curvature of the Earth has a negligible effect and can be assumed to be flat for frequencies less than 6 GHz over a smooth Earth [3]. The model was originally developed for antenna heights of 1 to 3 meters, but further improvements in the model have demonstrated that the model can be used for antenna height ranges from 0 to 1 meter. It is valid for frequencies from 150 MHz to 6000 MHz [2].

The space wave component (direct and reflected waves) and surface wave component of the ITS Undisturbed-Field Model are based on the Sommerfeld integral arising from the solution for the field due to an elemental dipole above a uniform, finitely-conducting, dielectric half space [4]–[6]. The half space is bounded by the Earth-air interface. Norton [4], [5], in his effort to simplify the expressions developed by Sommerfeld [7], derived equations that clearly show the surface wave and space wave components. Jordan [8] simplified Norton's equations by deleting the higher order terms for the vertical and radial directed components of the electric field in cylindrical coordinates. These higher order terms represent the induction and near field of the antenna and diminish rapidly with distance. Jordan [8] further reduced the equation complexity by combining the vector equations for the vertical and radial directed field components, and then separating the resulting equation into a total space (direct and reflected waves) and surface wave components. At distances within the line of sight, the field strength of the space and the surface wave for vertical polarization is given by [4], [5] and [8]:

$$E_{space} = i30IkL\left(\frac{e^{-ikr_1}}{r_1} + R_v \frac{e^{-ikr_2}}{r_2}\right)\cos\psi \tag{1}$$

$$E_{surface} = i30IkL\left(1-R_v\right)A\frac{e^{-ikr_2}}{r_2}\sqrt{1-2u^2+u^2\cos^2\psi\left(1+\frac{\sin^2\psi}{2}\right)}^2, \tag{2}$$

where:

$k = 2\pi/\lambda$,
A is the flat-Earth attenuation function,
I is the peak dipole current amplitude in amperes,
L is the length of the dipole in meters,
$u^2 = (\varepsilon_r\text{-}i\sigma/\omega\varepsilon_0)^{-1}$,
ω is the angular frequency and is equal to $2\pi f$,

f is the radio frequency in Hertz,
μ is the magnetic permeability of the Earth, $\mu = \mu_r \cdot 4\pi \cdot 10^{-7}$ henries per meter,
μ_r is the relative permeability of the Earth,
$\varepsilon = \varepsilon_r \cdot \varepsilon_0 = \varepsilon_r \cdot 8.85 \cdot 10^{-12}$ = the permittivity of the Earth in Farads per meter,
ε_r is the relative permittivity of the Earth,
ε_0 is the permittivity of free space in Farads per meter,
σ is the conductivity of the Earth in Siemens per meter,
ψ is the angle representing the direction of the incident wave measured with respect to the Earth's surface,
h_1 is the height of the transmitter antenna in meters,
h_2 is the height of the receiver antenna in meters,
d is the horizontal distance along the Earth.

The distance $r_1 = \left(d^2 + (h_1 - h_2)^2\right)^{1/2}$ is the distance between the dipole and the observation point in meters.

The distance $r_2 = \left(d^2 + (h_1 + h_2)^2\right)^{1/2}$ is the distance between the dipole image and the observation point in meters.

R_v is the complex reflection coefficient for vertical polarization and is given by:

$$R_v = \frac{\left(\varepsilon_r - i\frac{\sigma}{\omega\varepsilon_0}\right)\sin\psi - \sqrt{\left(\varepsilon_r - i\frac{\sigma}{\omega\varepsilon_0}\right) - \cos^2\psi}}{\left(\varepsilon_r - i\frac{\sigma}{\omega\varepsilon_0}\right)\sin\psi + \sqrt{\left(\varepsilon_r - i\frac{\sigma}{\omega\varepsilon_0}\right) - \cos^2\psi}} \tag{3}$$

Equations (1) through (3) are different for horizontal polarization and can be found in [8].

The attenuation function, *A*, is the ratio of the electric field from a short vertical dipole over the lossy Earth's surface to that field from the same short vertical dipole located on a flat perfectly conducting surface, and takes into account the ground losses. There are two forms of the attenuation function presented in this report. The ITS Undisturbed Field Model was developed in several versions, with each version improving on the previous versions. In response to a request from the NTIA Office of Spectrum Management, model development was initiated to specifically address the application of propagation loss predictions for very low antenna heights and close-in distances [2].

The original concept for development of a propagation model [2] used the Numerical Electromagnetic Code (NEC) software [12], which uses a method of moments technique in electromagnetics to compute the electric field versus frequency, ground constants, antenna heights, and distances. This electric field is then converted to a basic transmission loss as described in [2]. This original method was cumbersome and required running the NEC software

many times to get results over a variety of input parameters and scenarios to create lookup tables to cover the various parameter ranges. This was Version 0 of the ITS Undisturbed-Field Model.

Version 0 needed to be streamlined into a more efficient and flexible computation method in the form of a computer model that would rapidly compute propagation loss to be used in system performance computations and other analysis applications. In response to a Naval Research Laboratory request to further develop the initial concept into a fast efficient computation model, Version 1 was developed. The approximate attenuation function described by (4) and (5) is used in Version 1 of the Undisturbed-Field Model which is described in this section. It uses simple algebraic equations to perform the calculations. Version 2 uses the more exact representation of the attenuation function and is valid for a wider variety of parameters than Version 1. It uses a more complex mathematical algorithm to perform its computations when compared to the simple equations of Version 1. Version 2 contains the more precise form of the attenuation function that is used in the ITS Undisturbed-Field Model to perform the propagation loss computation in this analysis.

Version 1 of the ITS Undisturbed Field Model uses the original Norton approximation to the attenuation function. Norton simplified the exact and more complex equations for the surface wave attenuation function into two forms that are more amenable to calculation. Version 1 with the Norton approximations to the flat-Earth attenuation [4], [5] function of the surface wave can be easily implemented on a programmable calculator and is reasonably accurate for line-of-sight propagation [6].

The Version 1 attenuation function, *A*, is given by:

for $p_0 < 4.5$ and all b:

$$A = e^{-0.43 p_0 + 0.01 p_0^2} - \left(\sqrt{\frac{p_0}{2}}\right)(\sin b)\left(e^{\frac{-5}{8} p_0}\right) \tag{4a}$$

for $p_0 > 4.5$ and all b:

$$A = \frac{1}{2 p_0 - 3.7} - \left(\sqrt{\frac{p_0}{2}}\right)(\sin b)\left(e^{-\frac{5}{8} p_0}\right), \tag{4b}$$

where for vertical polarization:

$$\begin{aligned} p_0 &= \frac{\pi R(km)\left[f(MHz)\right]^2 \cos b}{\left(54x10^2\right)^2 \sigma} \\ b &= \tan^{-1} \frac{\left(\varepsilon_r + 1\right) f(MHz)}{18x10^3 \sigma} \end{aligned} \tag{5a}$$

and for horizontal polarization:

$$p_0 = \frac{\pi R(km) 6x10^4 \sigma}{\cos b}$$
$$b = \tan^{-1} \frac{(\varepsilon_r - 1) f(MHz)}{18x10^3 \sigma}, \quad (5b)$$

where:

$R(km) = r_2 \times 10^{-3}$ is the distance between the observation point and the dipole image in km,
σ is the conductivity of the Earth in Siemens per meter,
ε_r is the relative permittivity of the Earth,
f(MHz) is the frequency in MHz.

These results are approximations. More exact results were sought for implementation in the ITS Undisturbed-Field Model.

Version 2 uses Norton's more exact mathematical algorithm to compute the attenuation function for the more precise approximations ((6) and (7)) to the flat-Earth attenuation function. It is accurate for a wider range of parameters, but is more difficult to implement. This was derived by Norton from the original Sommerfeld formulation [7] for the flat-Earth attenuation function of the vertically polarized surface wave [5] and is given by:

$$A = \left| 1 + i\sqrt{\pi p_1} e^{-p_1} erfc\left(-i\sqrt{p_1}\right) \right|, \quad (6)$$

where

$$p_1 = -i\frac{k_2 r_2}{2}\Delta^2 \approx p_0 e^{i\left(b-\frac{\pi}{2}\right)} \quad (7a)$$

$$\Delta = \frac{1}{N}(1 + N\cos\theta_r) \quad (7b)$$

$$N = \frac{k_1}{k_2} = \left(\varepsilon_r - i\frac{\sigma}{\omega\varepsilon_0}\right)^{1/2} \quad (7c)$$

$$k_1 = \omega\sqrt{\mu_0\left(\varepsilon_r + i\frac{\sigma}{\omega}\right)}$$
$$k_2 = \omega\sqrt{\mu_0\varepsilon_0} \quad (7d)$$

$$r_2 = \left(d^2 + (h_1 + h_2)^2\right)^{1/2} \quad (7e)$$

$$\cos\theta_r = \frac{h_1 + h_2}{r_2}. \tag{7f}$$

The horizontal component of the surface wave attenuates at a rate several orders of magnitude greater than the vertical component and has a magnitude that is negligible in comparison to the vertically polarized component of the surface wave [8].

Equations (6) and (7) are implemented in Version 2 of the ITS Undisturbed-Field Model used for computation of the propagation losses. The complementary error function, designated by *erfc* in (6), is described in [9]. The parameters p_0 and b are as defined above (see (5a) and (5b)), and $i = \sqrt{-1}$.

The field strength at small distances is directly proportional to the square root of the power radiated by the transmitter and the directivity of the antenna in the horizontal and vertical planes. If the antenna is non-directional in the horizontal plane and has a vertical directional pattern that is proportional to the cosine of the elevation angle (this corresponds to a short vertical antenna), then the electric field at one kilometer for an effective radiated power of one kilowatt is 300 mV/m [1]. The flat-Earth attenuation function, A, depends on frequency, distance, and the ground constants of the Earth along which the wave is traveling. A numerical distance, p_0, and phase angle, b, can be computed and are functions of frequency, ground constants, and distance in wavelengths.

If the numerical distance, p_0, is less than one, then the attenuation function is very close to one, and, as a result, for distances close to the transmitting antenna the losses in the Earth have very little effect on the electric-field strength of the surface wave. In this region, the electric field strength is inversely proportional to distance. For situations where the numerical distance becomes greater than unity, the attenuation function rapidly decreases in magnitude. When the numerical distance becomes greater than 10, the attenuation factor is also inversely proportional to distance. In this circumstance, the combination of the attenuation factor and the un-attenuated electric field being inversely proportional to distance results in the electric field strength of the surface wave being inversely proportional to the square of the distance.

4 ELECTRIC FIELD PENETRATION DEPTH OF THE SOIL AND ITS EFFECT ON GROUND-WAVE PROPAGATION

The depth to which the ground currents and electric field penetrate below the Earth's surface and still maintain an appreciable magnitude is determined by the average values of the Earth conductivity (σ) and relative permittivity (ε_r), and the frequency. Penetration depth is similar to a skin depth phenomenon in a good conductor, but the Earth is a poor conductor. The skin depth ranges from a fraction of a meter at the highest frequencies for VHF communications to tens of meters at AM broadcast and lower frequencies. For this reason, ground-wave propagation at the lower frequencies is not particularly dependent on properties at the actual ground surface. Therefore, a recent rainfall which would result in a dramatic change of permittivity at the ground surface would not significantly affect propagation at MF and LF frequencies. However, at VHF frequencies a recent rainfall could affect the propagation of radio waves due to the additional moisture content of the ground near the ground surface.

The electric field strength at a distance z below the surface of the Earth is given by [10]:

$$E = E_0 e^{-\alpha z}, \tag{8}$$

where:

E_0 is the electric field intensity at the surface of the Earth,
z is the depth in meters below the surface of the Earth,
α is the attenuation per meter of the electric field intensity

The attenuation per meter α is given by:

$$\alpha = \omega\sqrt{\mu\varepsilon}\sqrt{\frac{1}{2}\sqrt{1+\left(\frac{\sigma}{\omega\varepsilon}\right)^2}-\frac{1}{2}}, \tag{9}$$

where:

ω is the angular frequency and is equal to $2\pi f$,
f is radio frequency in Hertz,
μ is the magnetic permeability of the Earth $\mu = \mu_r \cdot 4\pi \times 10^{-7}$ Henries per meter,
μ_r is the relative permeability,
ε = the permittivity of the Earth = $\varepsilon_r \cdot (8.85 \times 10^{-12})$ Farads per meter,
ε_r is the relative permittivity of the Earth,
σ is the conductivity of the Earth in Siemens per meter.

The distance the wave must travel in a lossy medium to reduce its amplitude to e^{-1} =0.368 of its value at the surface is $\delta = 1/\alpha$ meters and is called the skin depth of the lossy medium. For other values of attenuation of the electric field, $r=e^{-\alpha z}$, one can use α to determine the distance z below the surface where the electric field is attenuated to that ratio r. The ratio r is always less than or equal to 1. The distance z is given by:

$$z = -\frac{ln\, r}{\alpha}, \tag{10}$$

where *lnr* is the natural logarithm of *r*.

An example is where f=300 kHz, μ_r = 1 for a nonmagnetic Earth, ε_r = 15 for average ground, σ = .005 for average ground. The attenuation α is calculated as .0751 per meter and δ is calculated as $1/\alpha$ = 13.32 meters.

The skin depth is the distance at which the electric field is e^{-1} or .368 (36.8 percent) of its value at the surface of the Earth [10]. The electric field at this large percentage does not represent a significant attenuation of the electric field. Some applications may require a lower electric field percentage such as 10 percent. If the distance, z, at which the electric field is .1 (10 percent) of its value at the surface is desired, then *ln r* is *ln* (.1) = -2.3026, and α = .0751, so $z = -(-2.3026)/\alpha = 30.66$ meters. Figure 4 shows the skin depth of several types of media as a function of frequency. The skin depth does not vary by significant amounts for each media type at these frequencies. Figure 4 demonstrates how significant the different ground constants are in affecting the magnitude of the skin depth. It shows that the skin depth is quite large for poor and average ground. Figure 5 is an expansion of Figure 4 along the frequency axis to show the skin depth in the 100 kHz to 10 MHz range, and demonstrates how large the skin depths are below 2 MHz.

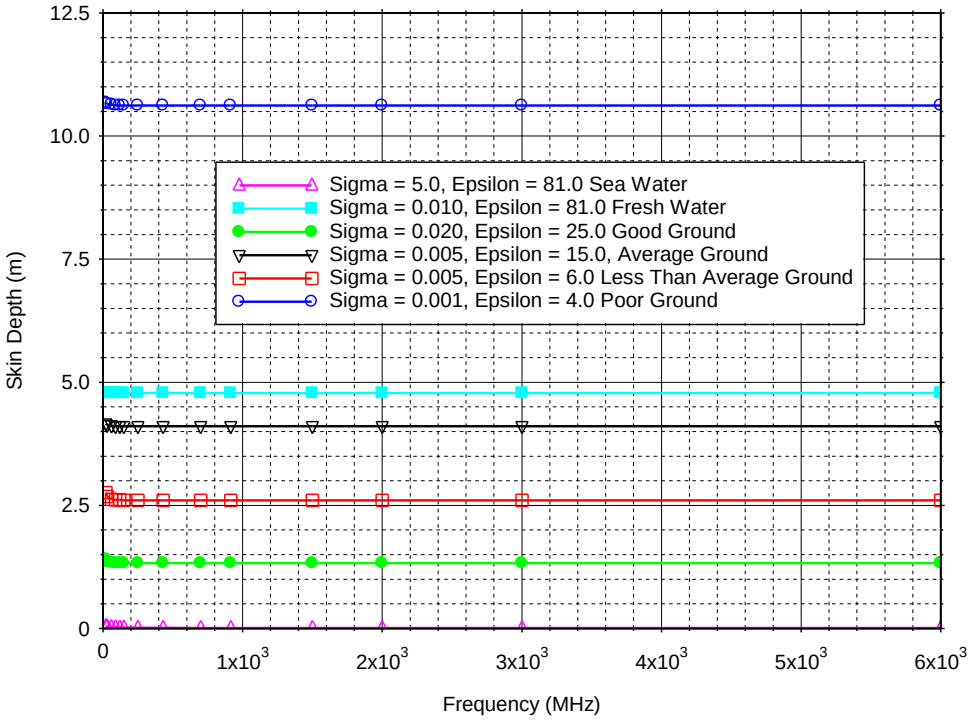

Figure 4. Skin depth for 1/e E-field attenuation versus frequency for various media types.

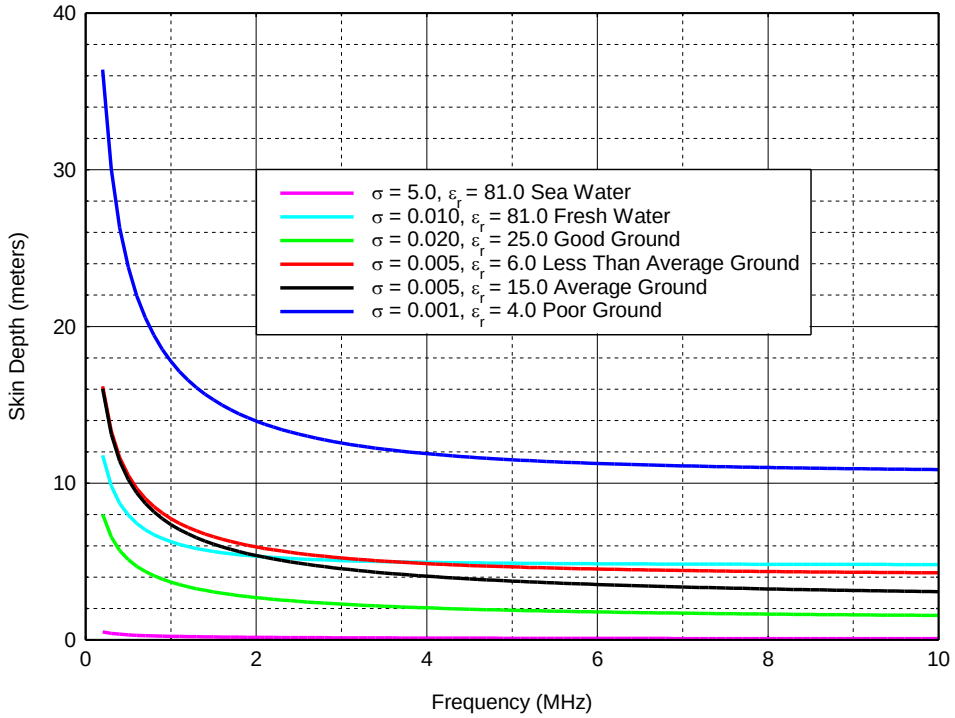

Figure 5. Skin depth for 1/e E-field attenuation versus frequency for various media types for lower frequencies.

4.1 Computed Sensitivity of Propagation Loss to Values of Epsilon (ε_r) and Sigma (σ)

The Undisturbed-Field Model [2] developed at ITS was used to perform all propagation loss prediction computations as a function of antenna heights, relative dielectric constant (ε_r), conductivity (σ), frequency, and distance. The results of these computations are shown in the figures in Appendix A. The model has been verified with comparisons to more exact models [2] and measured data.

Figure A-1 shows the propagation loss for three types of ground for a distance of 10 meters for antenna heights at zero meters. There is a significant difference in the predicted propagation loss between poor ($\varepsilon_r = 4.0$, $\sigma = 0.001$) and good ground ($\varepsilon_r = 25.0$, $\sigma = 0.020$). As part of this analysis effort, a study was performed to determine the sensitivity of the propagation loss to variations in conductivity (σ) and relative permittivity (ε_r). Figures A-2 through A-5 show the sensitivity of propagation loss to σ and ε_r for a separation distance of 10 meters. The heights of the transmitter and receiver antennas for all figures in the Appendix are equal to zero. The computations and measurements are based on heights of 8.9 centimeters which is equivalent to a zero height at these frequencies. Computations at heights of 8.9 centimeters and 0.0 centimeters verify this assumption. Figure A-2 shows that for a low conductivity, the loss is very dependent on the value of ε_r, but Figure A-3 shows that for a higher σ the loss has less dependence on ε_r, particularly for frequencies at and below 150 MHz. Figures A-4 and A-5 show that the loss is dependent on σ only for frequencies at and below 150 MHz. The sensitivity to variation in σ is greater for lower values of ε_r. Figure A-4 has a value of $\varepsilon_r = 4$ and a higher sensitivity to changes in σ, whereas Figure A-5 has a value of $\varepsilon_r = 25$ and a much lower sensitivity to variations in σ. Figure A-6 is a plot of loss versus σ with an expanded scale and shows how insensitive the loss is to variations in σ for frequencies above 150 MHz. Figure A-6 shows that there is some capability to determine σ from lower frequency data at and below 150 MHz.

5 SOIL DIELECTRIC PROPERTIES OBTAINED AT TABLE MOUNTAIN USING MONOPOLE TRANSMISSION MEASUREMENTS

Figures A-7 through A-11 show the results of comparing predictions to measurements for data taken in late August of 2009. The distance and vertical scales were expanded for better vertical scale resolution. Measured data was originally recorded over separation distances ranging from 2 to 250 meters using monopole antenna pairs resonant at the five frequencies (150.5, 250, 430, 700 and 915 MHz). The data show that the dielectric constants vary over the distance of the measurement path. Most data analysis took place over shorter distances. This study concentrated on distances in the 5 to 15 meter range. The ground at Table Mountain is not homogeneous, which accounts for the erratic variation of loss versus distance shown in Figures A-7 through A-11.

These data were available to determine the ground parameters of σ and ε_r for the measured data collected in August 2009. Since the values of σ could not be determined at the frequencies above 150 MHz as discussed in Section 3.1, only ε_r was obtained from these plots. This is due to the lack of sensitivity of the propagation loss at or above 150 MHz to values of σ. At lower frequencies below 150 MHz, the loss is insensitive to variations in ε_r, but sensitive to variations in σ. The permittivity varies as a function of distance and frequency. Table 1 shows the results of extracting the values of permittivity from Figures A-7 through A-11 (August 2009 data) for a conductivity of $\sigma = 0.005$ Siemens per meter. Table 2 shows the values of σ from Figures A-12 through A-19 (August 2009 data). The average value of ε_r in Table 1 is approximately 6.0 for the first three values of Table 1 and 7.0 for the entire table, so the values of ε_r of 6.0 to 7.0 were used to determine σ, because ε_r is known to be relatively constant in the 30 to 150 MHz region [11]. Referring to Figures A-2 and A-3 the loss versus ε_r curves are relatively flat between $\varepsilon_r = 6.0$ and 7.0 for frequencies less than 150 MHz.

Table 1. Values of permittivity (ε) for the distance range of 8 to 10 meters at frequencies at and above 150.0 MHz (August 2009 data).

Frequency (MHz)	**Permittivity, ε_r**	**Conductivity, σ (S/m)**
150.5	7.0 to 8.0	0.005
250.0	6.0 to 7.0	0.005
430.0	4.0 to 5.0	0.005
700.0	7.0 to 9.0	0.005
915.0	8.0 to 9.0	0.005

The analysis using the lower frequencies below 150 MHz was performed to determine σ by compensating the measured data to take into account the reduced efficiency of the antennas when operating below 150 MHz and then comparing these measured data to the predictions at these lower frequencies. The distance range was reduced to 7 to 9 meters to allow expansion of the vertical scales for better resolution.

Using data at lower frequencies below 150 MHz, this compensation technique was used to extract σ, from the measured data shown in Figures A-12 to A-19. The monopole antennas are narrowband and resonant at their design frequencies. The raw measured data shows the maximal response of these antennas at their resonant frequencies. The compensation technique included a correction by applying an impedance mismatch loss in addition to an adjustment of average gain at the lower frequencies.

This mismatch and gain compensation information was obtained by modeling the 150 MHz monopole antennas at frequencies below 150 MHz using the method of moments technique of the NEC software [12]. The NEC software can compute an antenna's radiation pattern, gain, and input impedance characteristics. The physical and electrical structure of the 150 MHz resonant monopole on a circular ground plane was used as input to the NEC software. When this antenna is analyzed at frequencies other than 150 MHz with the NEC software, the gain, input impedance, and radiation pattern are computed at the other frequencies computed.

The mismatch loss was computed from the computed input impedance using conventional techniques as found in [8]. The total degradation in gain and efficiency at frequencies below 150 MHz was obtained by adding the gain degradation and the impedance mismatch loss. Using the 150 MHz monopole provided useful data down to 30 MHz. The results from Figures A-12 through A-19 are summarized in Table 2 for the frequencies listed.

Table 2. Values of ε_r for the various distances, frequencies, and permittivity for the distance range of 8 to 10 meters for frequencies below 150 MHz (August 2009 Data).

Frequency (MHz)	**Permittivity, ε_r**	**Conductivity, σ (S/m)**
30.0	6.0	0.005
60.0	6.0	0.009
30.0	6.5	0.005
60.0	6.5	0.007
30.0	6.7	0.004
60.0	7.0	0.007
30.0	7.0	0.004
60.0	7.0	0.006

A second set of measured data was recorded in May 2010 using the same stepped frequency technique using sets of monopole antennas resonant at 150.5, 250, 430, 700, and 915 MHz, but only at a single distance of 8.3 meters. A limited amount of data was available from these measurements. It was determined that the relative permittivity (ε_r) and conductivity (σ) were higher for this set of measurements. The results of these May 2010 measurements are shown in Figures A-20 through A-24, which are expanded plots for better resolution. These figures were used to determine ε_r of the ground at and above 150 MHz. Table 3 summarizes the values of ε_r extracted from Figures A-20 through A-24 for $\sigma = 0.005$ Siemens/meter.

Table 3. Values of ε_r at different frequencies at a distance of 8.3 meters (May 2010 data).

Frequency (MHz)	**Permittivity, ε_r**	**Conductivity, σ (S/m)**
150.5	9.0 to 10.0	0.005
250.0	10.0	0.005
430.0	7.5	0.005
700.0	9.0	0.005
915.0	9.0	0.005

These values of ε_r from Figures A-20 through A-24 were used to determine the conductivity in Figures A-25 through A-29 at frequencies below 150 MHz.

The higher values for ε_r of the May 2010 data when compared to measurements of the previous year (August 2009) were thought to be a result of increased moisture content due to the heavier rainfall that occurred prior to the May 2010 measurements. Soil conditions were drier when the previous measurements were taken, in August 2009. For both sets of measurements the ground was not homogeneous, but this surface wave technique of determining the ground constants results in an aggregate measure of the non-homogeneous ground at Table Mountain.

Figures A-25 through A-29 present the results of comparing the May 2010 measured data to the predictions, with plots expanded for better resolution. These figures were used to determine σ of the ground for the second set of measurements using the lower frequency compensation technique described previously at frequencies below 150 MHz, since σ could not be resolved from the measurements above 150 MHz. The plots in these Figures are expanded with better vertical scale resolution to facilitate the extraction of data. Table 4 summarizes the results of extracting the values of σ from Figures A-25 through A-29. Referring to Figures A-2 and A-3 the loss versus ε_r curves are relatively insensitive to changes in ε_r between $\varepsilon_r = 7.0$ to 9.0, which were the ε_r values used in Table 4 for determining σ.

Table 4. Values of conductivity and permittivity, for various frequencies for the single distance of 8.3 meters (May 2010 data).

Frequency (MHz)	**Permittivity, ε_r**	**Conductivity, σ (S/m)**
30.0	7.0	0.008
30.0	7.5	0.006
30.0	8.0	0.005
90.0	7.0	0.005
120.0	9.0	0.007

6 CONCLUSION

It was determined that the propagation loss of the surface wave is relatively insensitive to σ (the conductivity), but does show significant variation with respect to ε_r (the relative dielectric constant) for frequencies including and above about 150 MHz. Lower frequencies below 150 MHz do show some variation with σ, and small variations at these lower frequencies can be used to determine σ. At higher frequencies, the variation of propagation loss could not be used to determine σ. This method can be used as a comparison to a vertical incidence (reflection coefficient) measurement/analysis effort that is currently underway, and could provide possible verification of values of ε_r obtained with the vertical incidence method.

Future work would include examining these data above and below 150 MHz using a computer program with an optimization algorithm to determine the values of ε_r and σ. Another area of future work would include developing a method that would use the phase angle of the transfer function S_{21} from the measured data with a propagation loss prediction algorithm that contains phase angle as an alternative method of obtaining the σ from data at frequencies above and below 150 MHz. Separation of the transfer function into real and imaginary components could provide better resolution for determination of the σ for comparison to the mathematical expressions for propagation loss of the surface wave.

7 REFERENCES

[1] F.E Terman, *Electronic and Radio Engineering,* New York: McGraw-Hill Book Co., 1955, pp.803–808.

[2] N. DeMinco, "Propagation loss prediction considerations for close-in distances and low-antenna height applications," NTIA Report TR-07-449, July 2007.

[3] A. Picquenard, *Radio-Wave Propagation,* New York: John Wiley& Sons, 1974, p.80.

[4] K.A. Norton, "The calculation of ground-wave field intensity over a finitely conducting spherical Earth," *Proceedings of the Institute of Radio Engineers,* Vol. 29, No. 12, December 1941, pp 623–639.

[5] K.A. Norton, "The propagation of radio waves over the surface of the Earth and in the upper atmosphere," Part I, *Proc. IRE,* Vol. 24, Oct. 1936, pp 1367–1387; Part II, *Proc. IRE,* Vol. 25, Sept. 1937, pp. 1203–1236.

[6] R. Li. "The accuracy of Norton's empirical approximations for ground-wave attenuation," *IEEE Trans. Ant. Prop.*, AP-31, No. 4, pp. 624-628, July 1983.

[7] A. Sommerfeld, "Propagation of waves in wireless telegraphy," Ann. D. Phys. 28, pp.665-736, March 1909.

[8] E.C. Jordan, *Electromagnetic Waves and Radiating Systems,* New Jersey: Prentice Hall, 1968, pp.628–650.

[9] M. Abramowitz and I.A. Stegun, *Handbook of Mathematical Functions, National Bureau of Standards AMS 55,* U.S. Government Printing Office: Washington, D.C., June 1964, pp. 297–329.

[10] C.A. Balanis, *Advanced Engineering Electromagnetics*, New York: John Wiley and Sons, 1989, pp.145–154.

[11] International Telecommunications Union (ITU-R), "Electrical characteristics of the surface of the Earth," ITU-R Recommendation P.527-3, 1992.

[12] G.J. Burke, "Numerical Electromagnetics Code- NEC-4, method of moments Parts I and II," University of California Lawrence Livermore Laboratory Report UCRL-MA-109338, Livermore, California, 1983.

APPENDIX A FIGURES SHOWING RESULTS OF COMPUTATIONS AND MEASUREMENTS FOR DIELECTRIC CONSTANT AND CONDUCTIVITY DETERMINATION WITH ALL ANTENNA HEIGHTS EQUAL TO ZERO

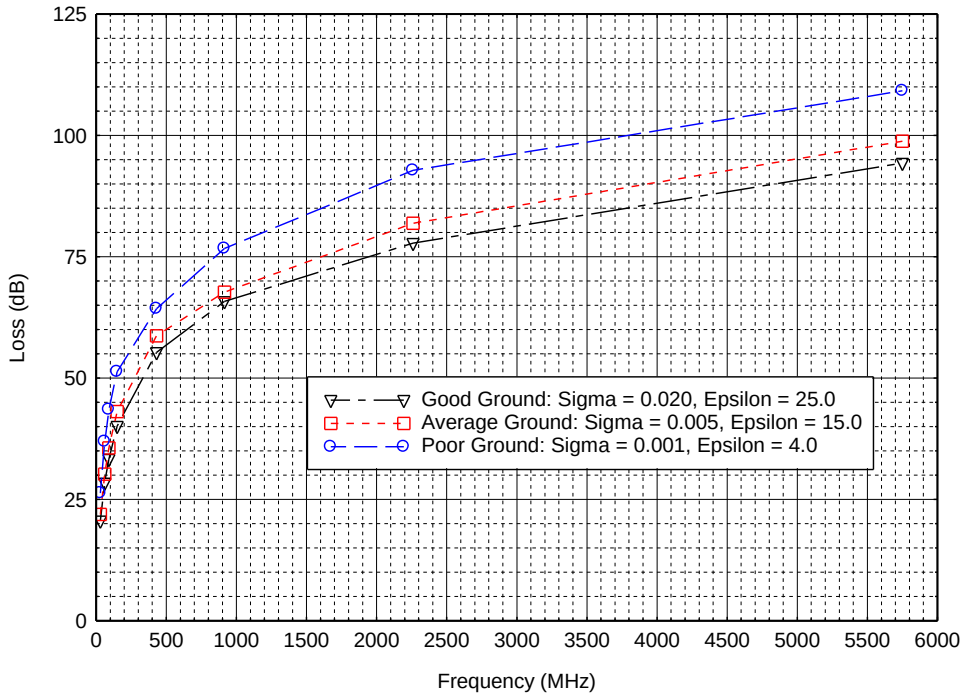

Figure A-1. Propagation loss versus frequency for three types of ground for a distance of 10 meters.

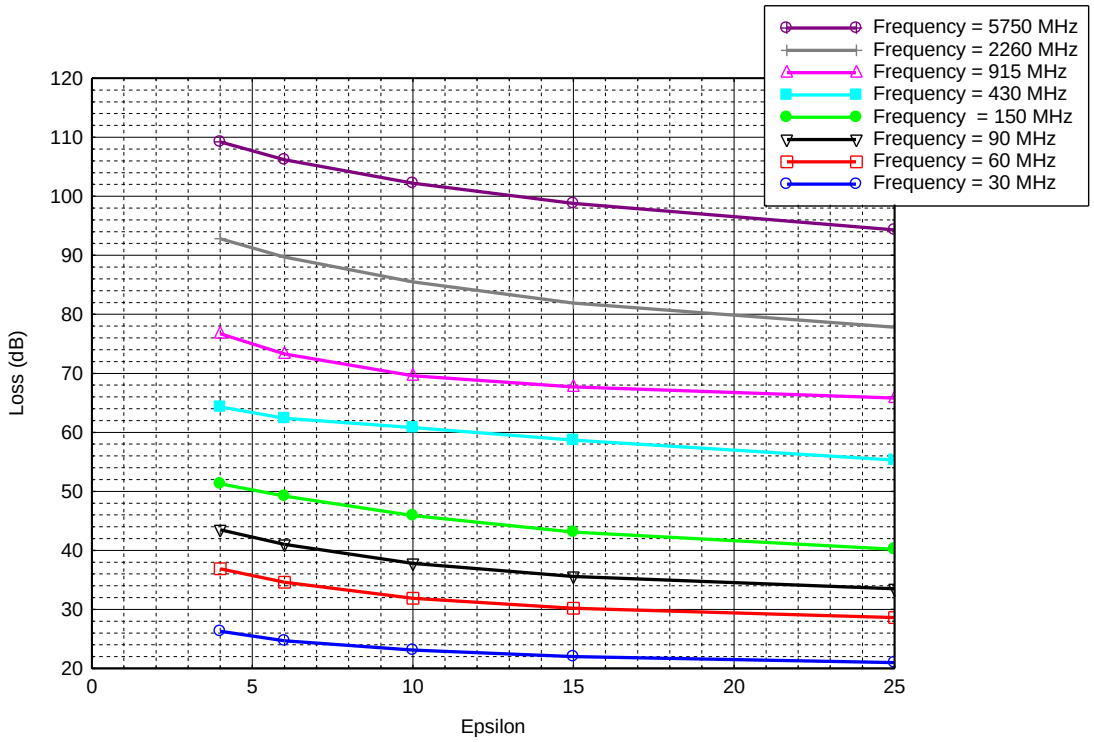

Figure A-2. Propagation loss versus epsilon for sigma = 0.001 and distance = 10.0 meters with frequency as a parameter.

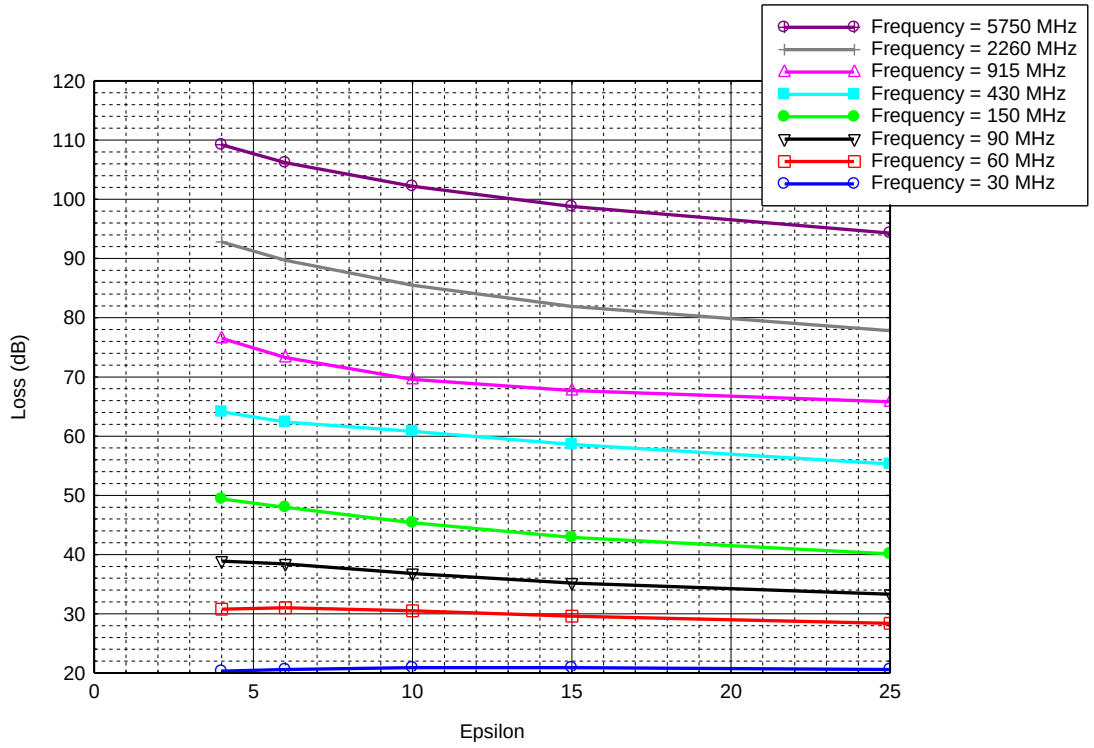

Figure A-3. Propagation loss versus epsilon for sigma 0.020 and distance = 10.0 meters with frequency as a parameter.

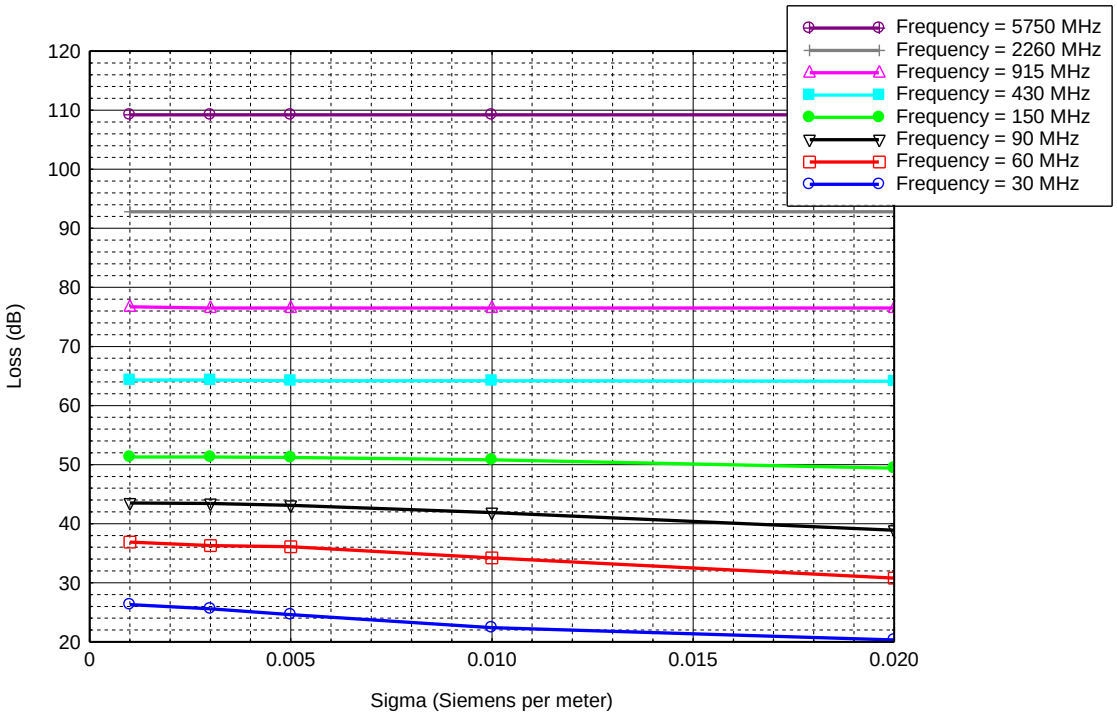

Figure A-4. Propagation loss versus sigma for epsilon = 4.0 and distance = 10.0 meters with frequency as a parameter.

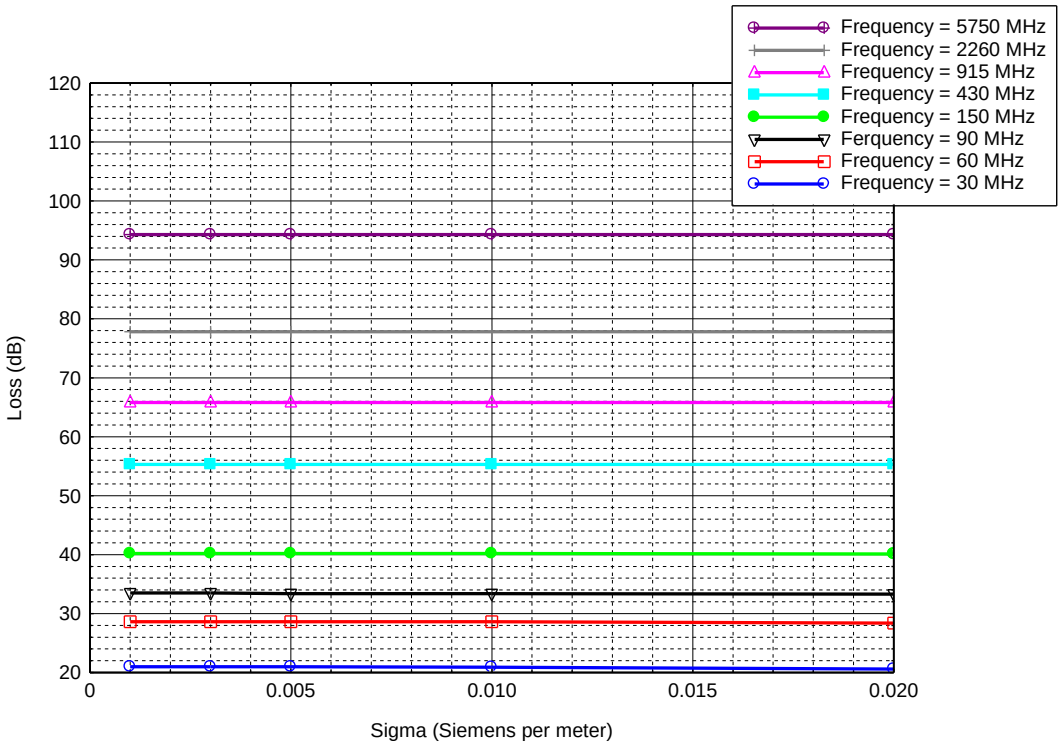

Figure A-5. Propagation loss versus sigma for epsilon = 25.0 and distance = 10.0 meters with frequency as a parameter.

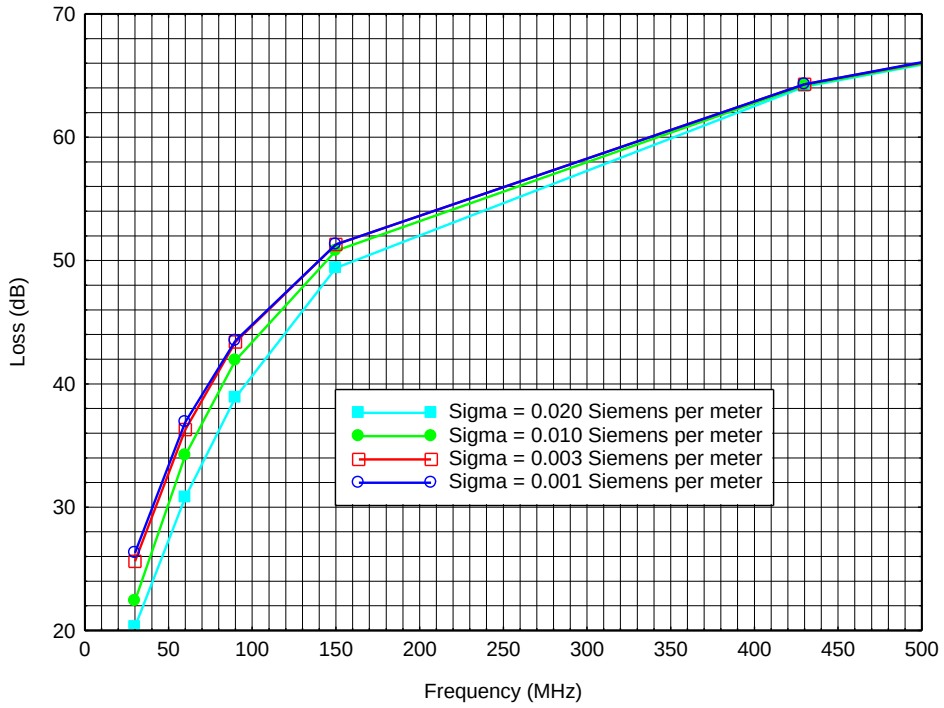

Figure A-6. Propagation loss versus frequency for epsilon = 4.0 with sigma as a parameter for a distance of 10 meters with all curves merging together.

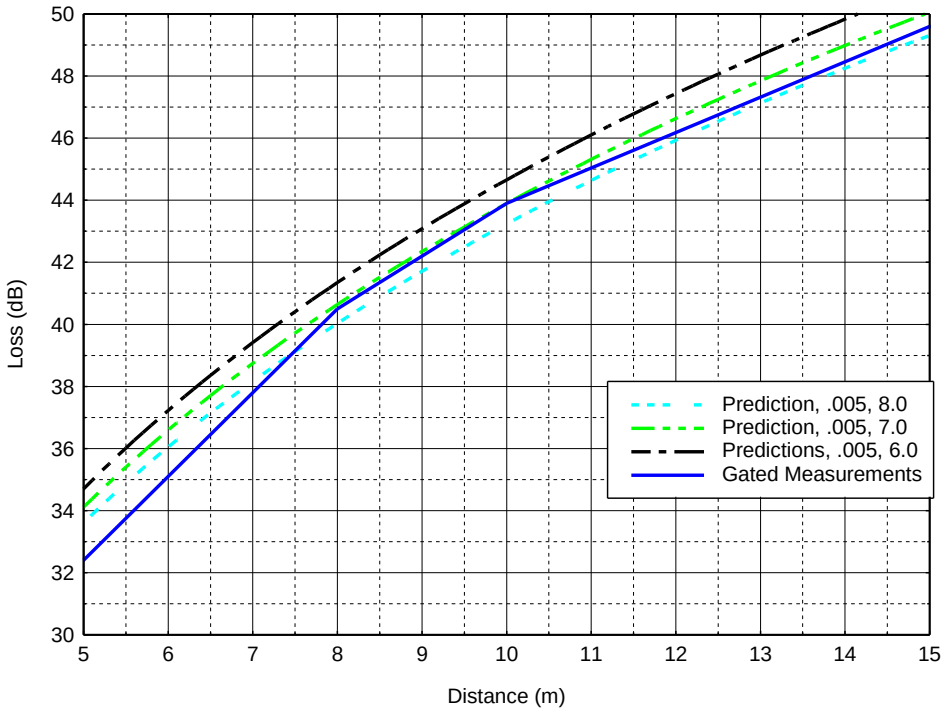

Figure A-7. Comparisons of propagation loss predictions with monopole measurements (August 2009) at 150.5 MHz.

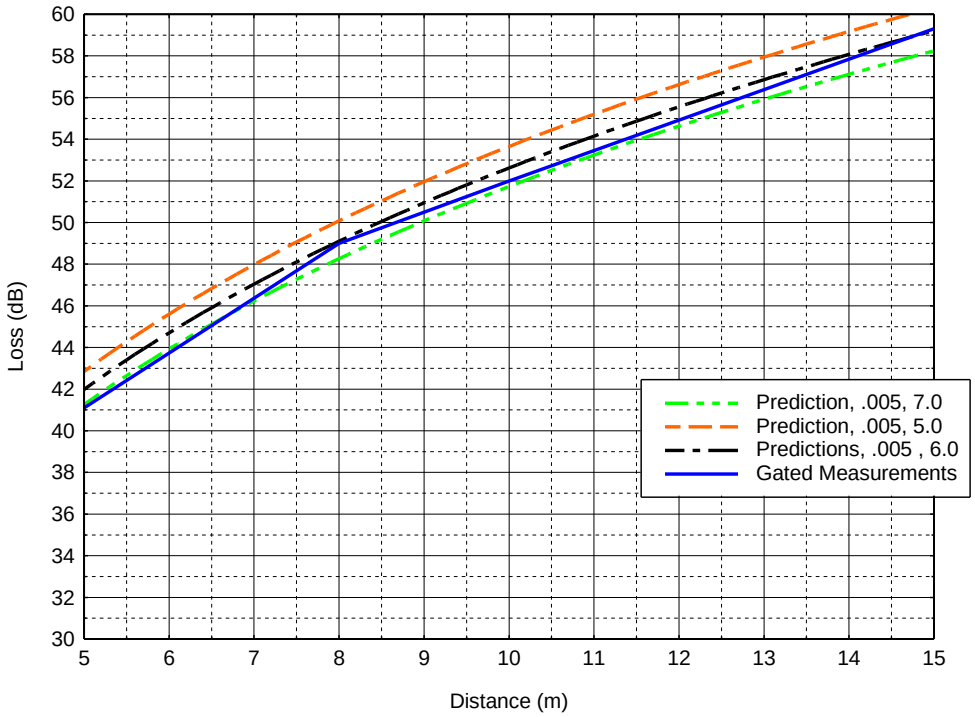

Figure A-8. Comparisons of propagation loss predictions with monopole measurements (August 2009) taken at 250 MHz.

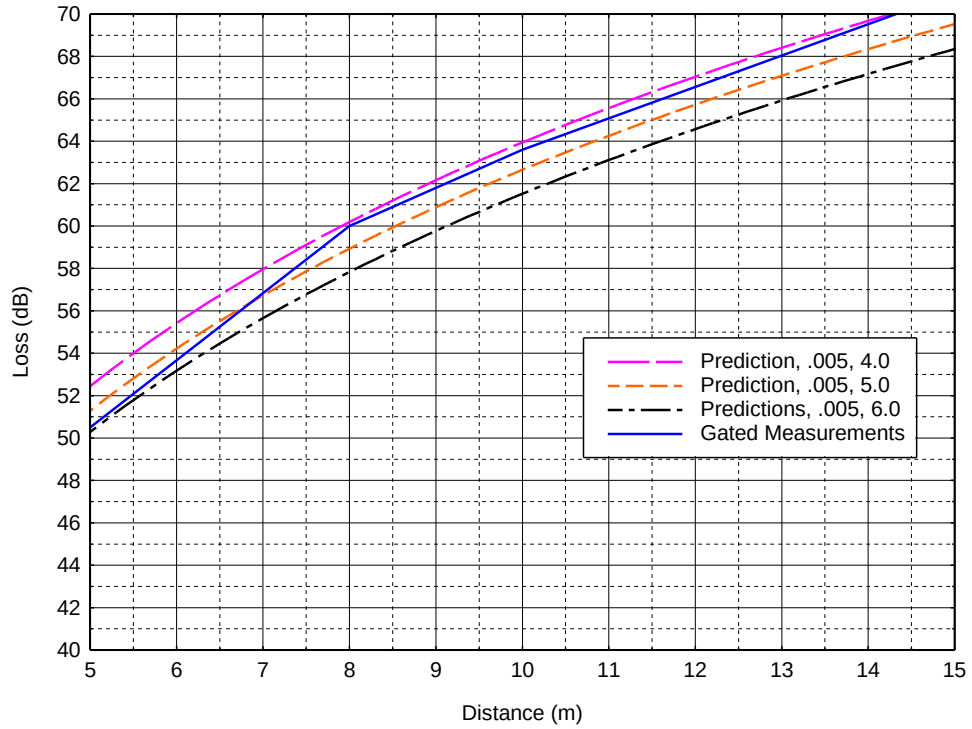

Figure A-9. Comparisons of propagation loss predictions with monopole measurements (August 2009) taken at 430 MHz.

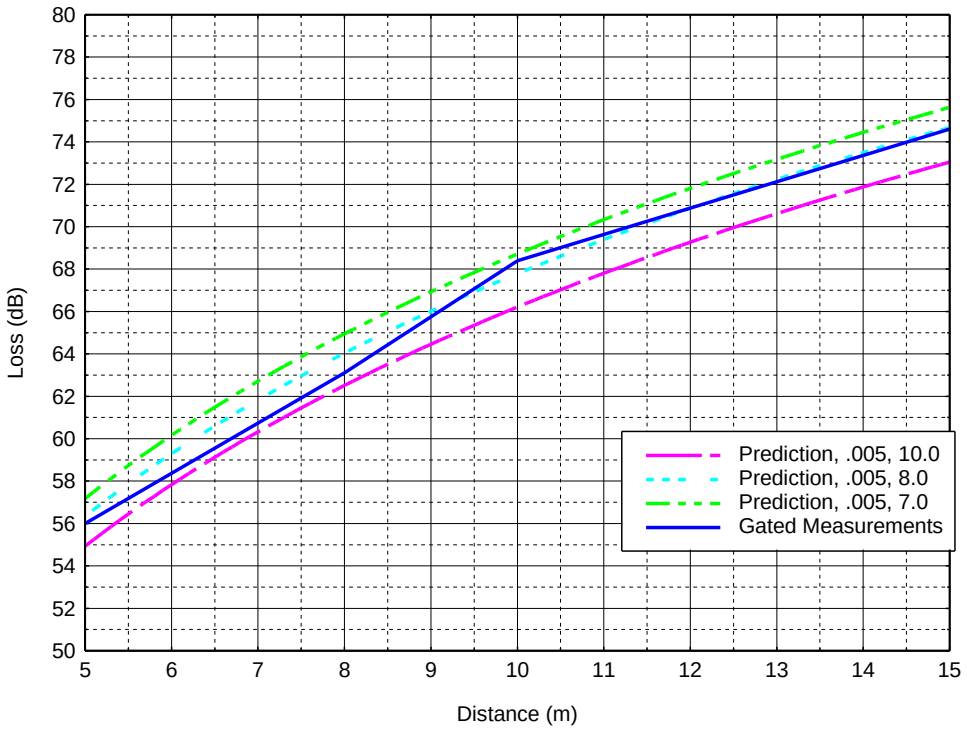

Figure A-10. Comparisons of propagation loss predictions with monopole measurements (August 2009) at 700 MHz.

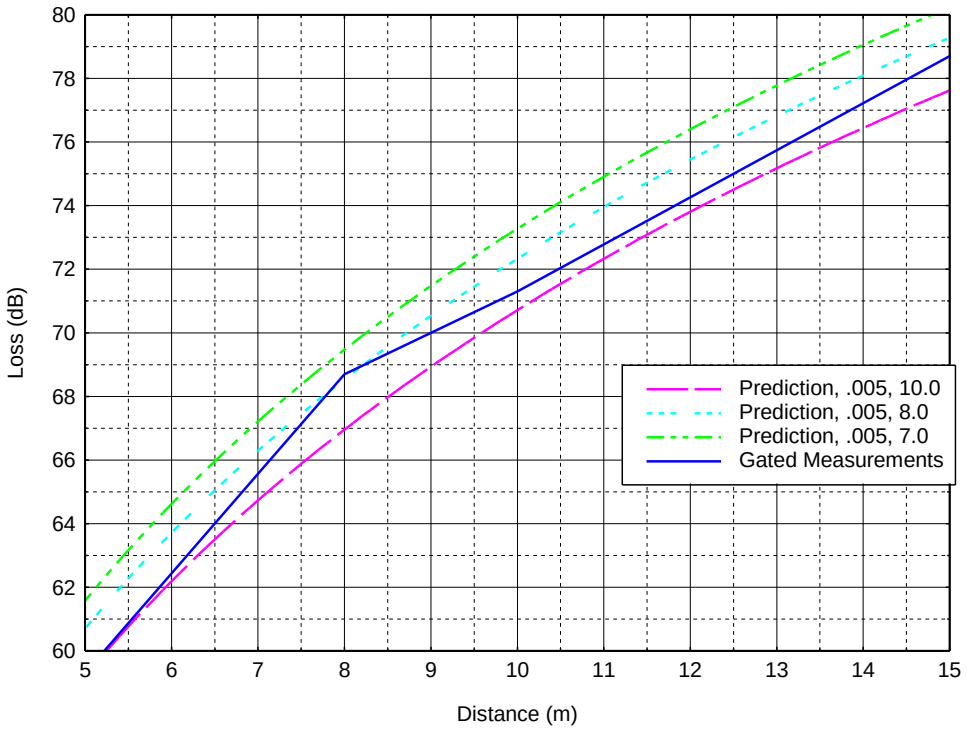

Figure A-11. Comparisons of propagation loss predictions with monopole measurements (August 2009) at 915 MHz.

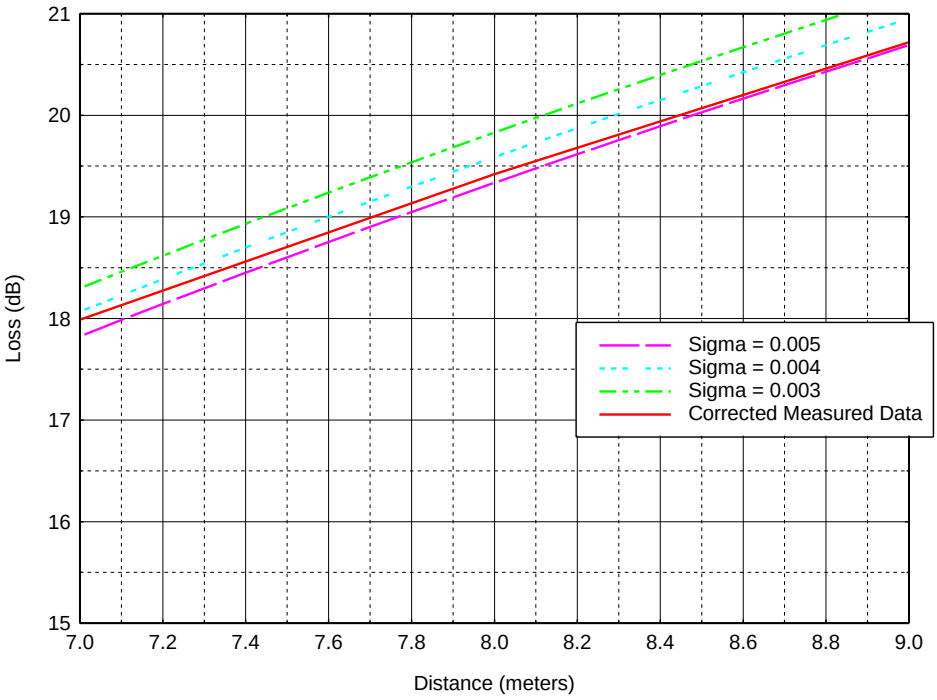

Figure A-12. Corrected measured propagation loss data (August 2009) versus distance compared to predicted loss for 30 MHz with $\varepsilon_r = 6.0$ and σ as a parameter.

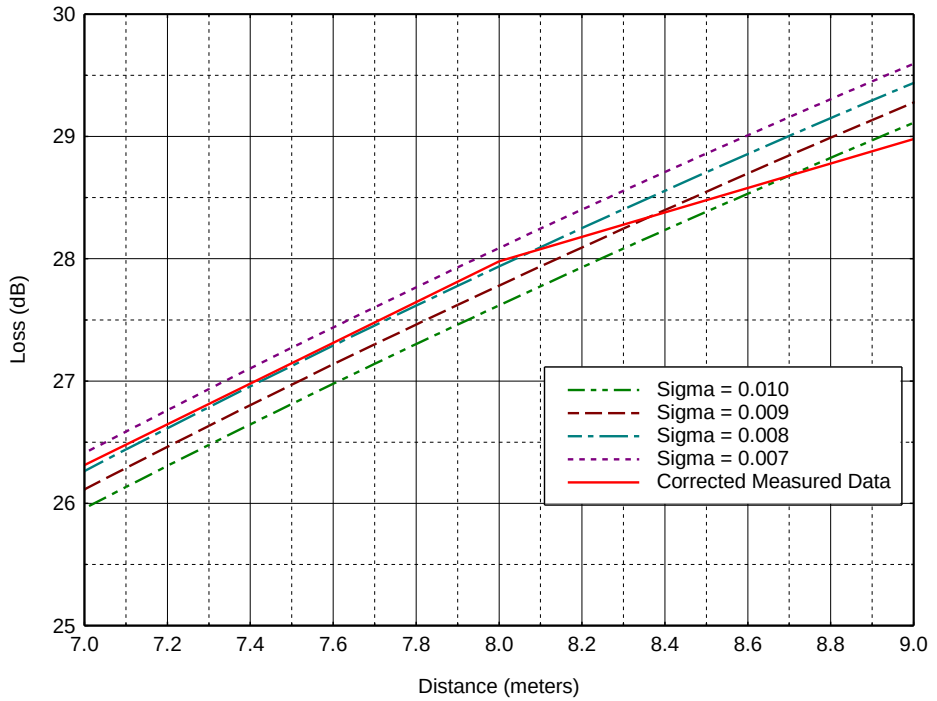

Figure A-13. Corrected measured propagation loss data (August 2009) versus distance compared to predicted loss for 60 MHz with $\varepsilon_r = 6.0$ and σ as a parameter.

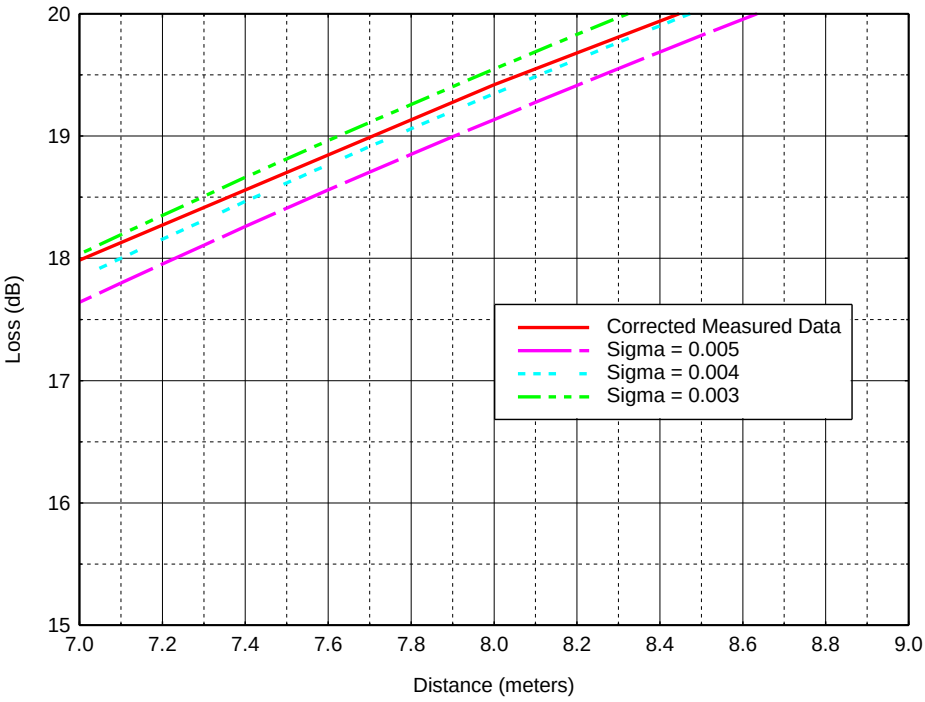

Figure A-14. Corrected measured propagation loss data (August 2009) versus distance compared to predicted loss for 30 MHz with $\varepsilon_r = 7.0$ and σ as a parameter.

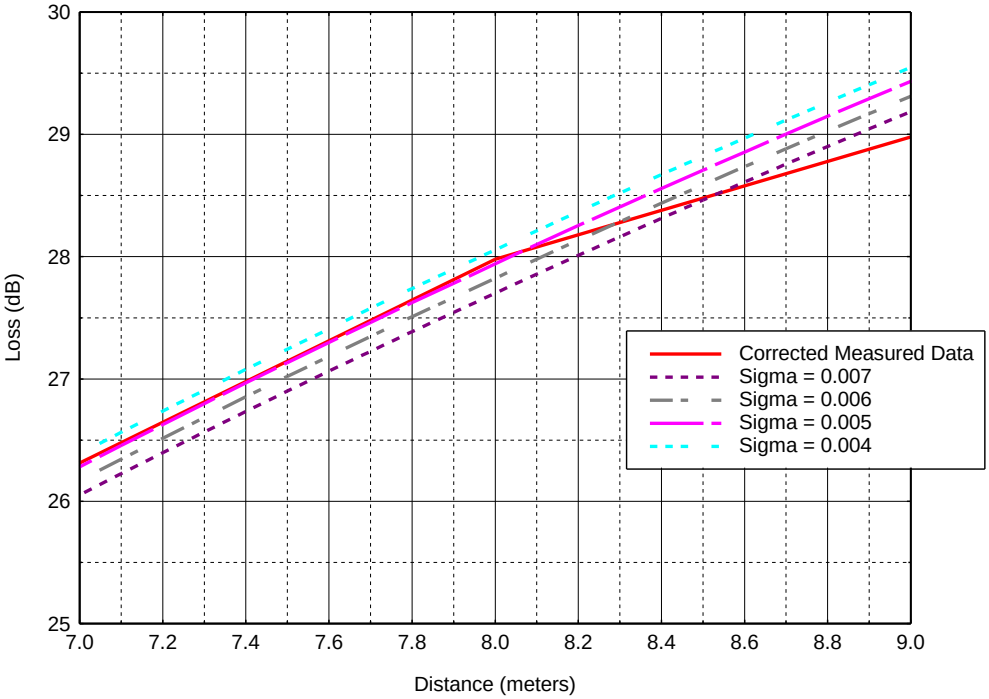

Figure A-15. Corrected measured propagation loss data (August 2009) versus distance compared to predicted loss for 60 MHz with $\varepsilon_r = 7.0$ and σ as a parameter.

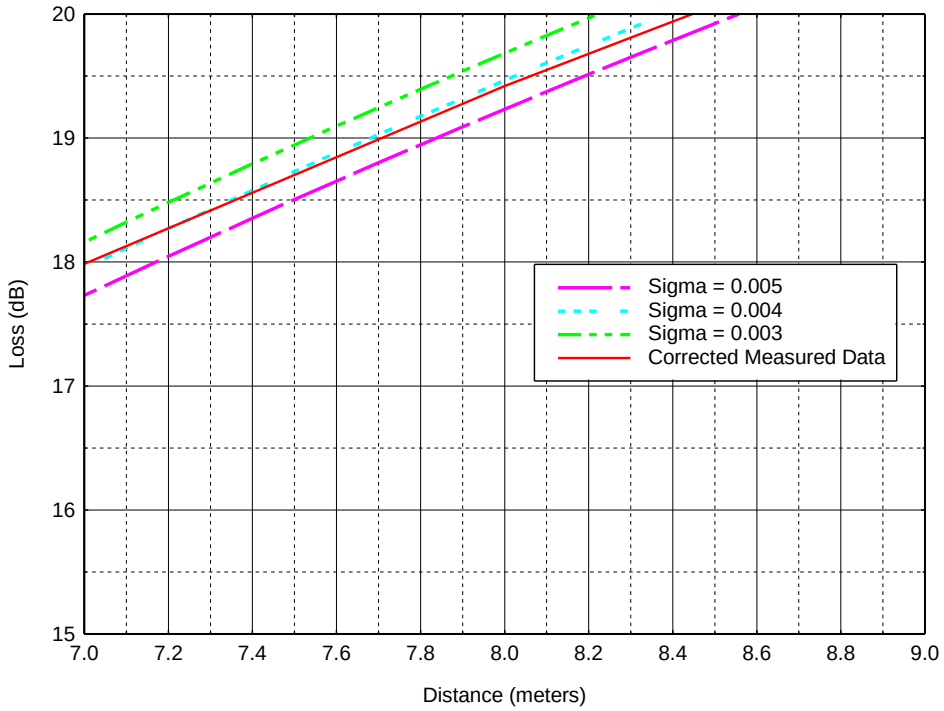

Figure A-16.Corrected measured propagation loss data (August 2009) versus distance compared to predicted loss for 30 MHz with $\varepsilon_r = 6.5$ and σ as a parameter.

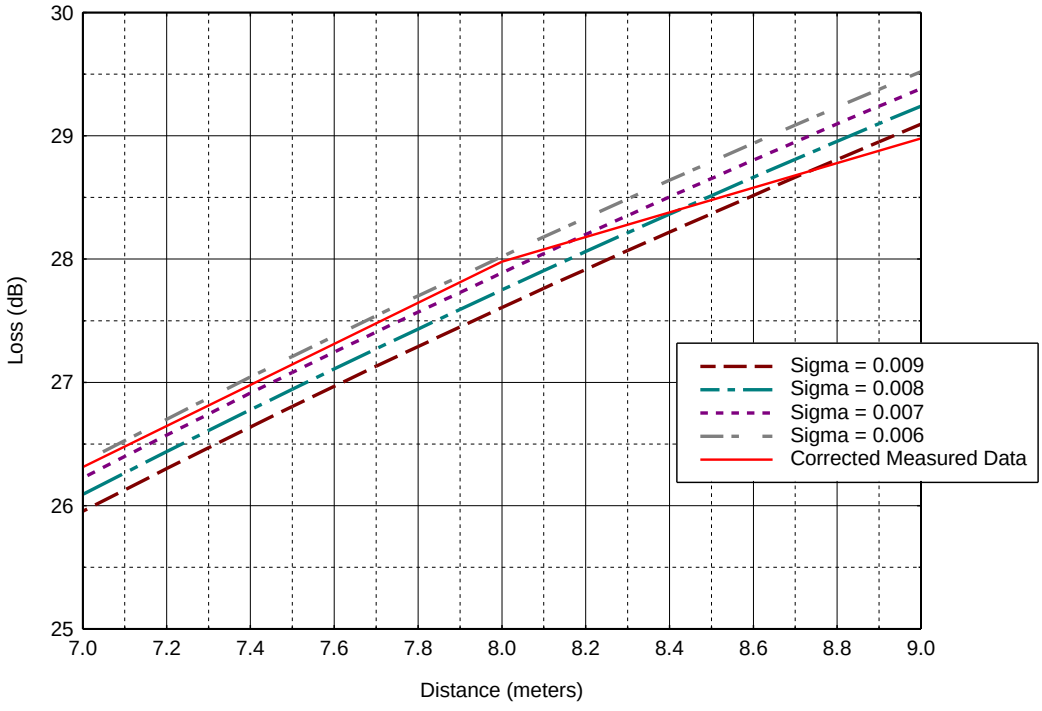

Figure A-17. Corrected measured propagation loss data (August 2009) versus distance compared to predicted loss for 60 MHz with $\varepsilon_r = 6.5$ and σ as a parameter.

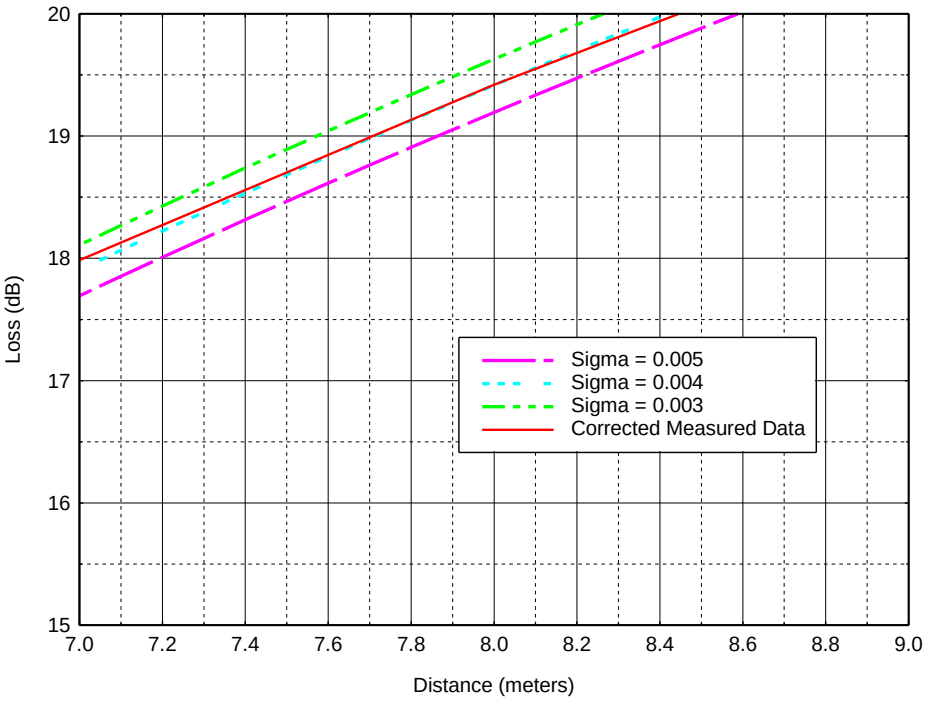

Figure A-18. Corrected measured propagation loss data versus distance compared to predicted loss for 30 MHz with $\varepsilon_r = 6.7$ and σ as a parameter.

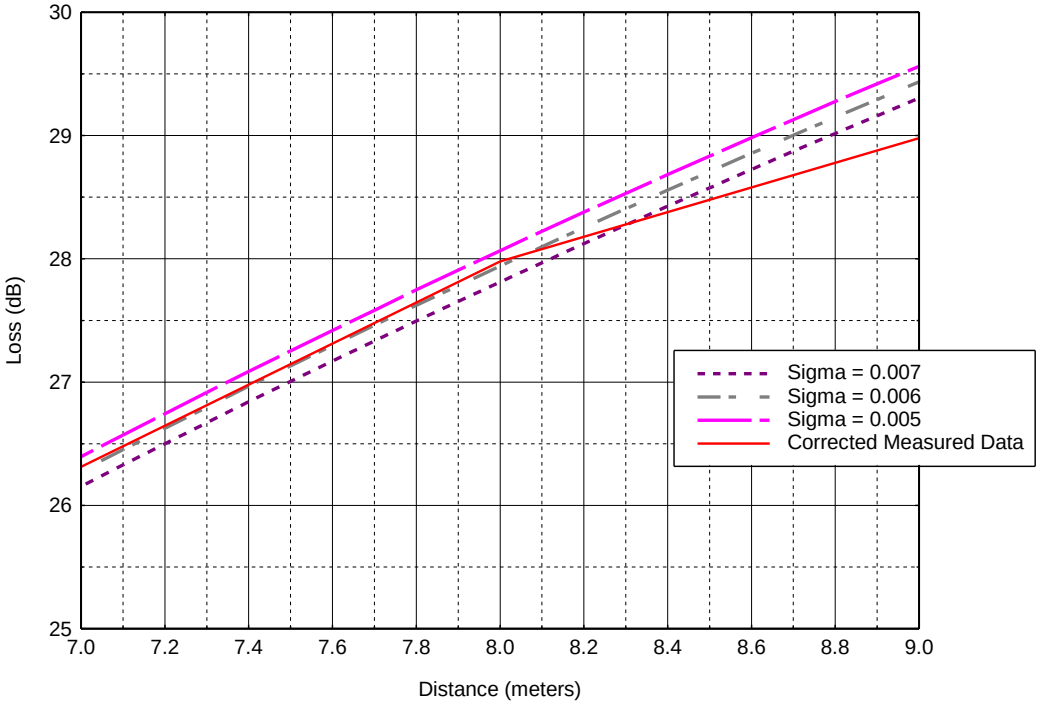

Figure A-19. Corrected measured propagation loss data (August 2009) versus distance compared to predicted loss for 60 MHz with $\varepsilon_r = 6.7$ and σ as a parameter.

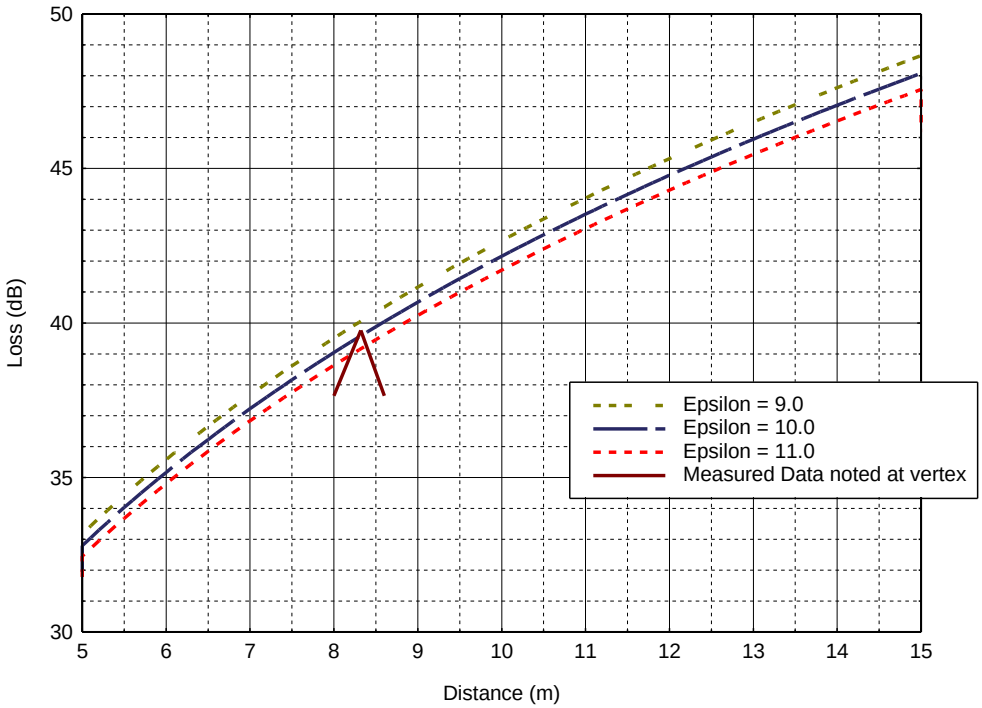

Figure A-20. Comparisons of propagation loss predictions with monopole measurements (May 2010) at 150 MHz with $\sigma = 0.005$.

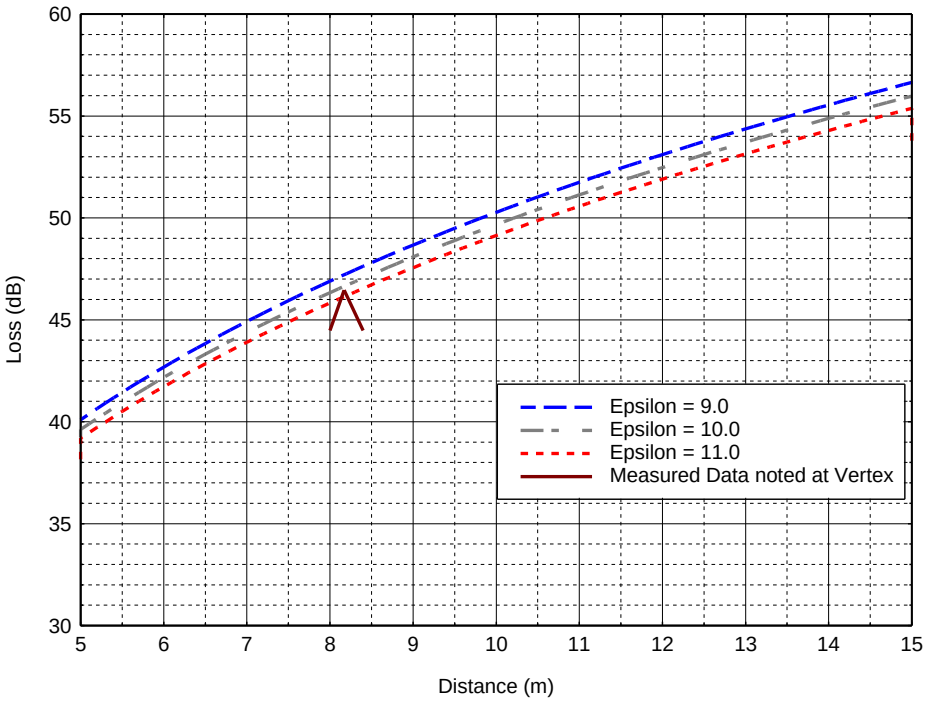

Figure A-21. Comparisons of propagation loss predictions with monopole measurements (May 2010) at 250 MHz with $\sigma = 0.005$.

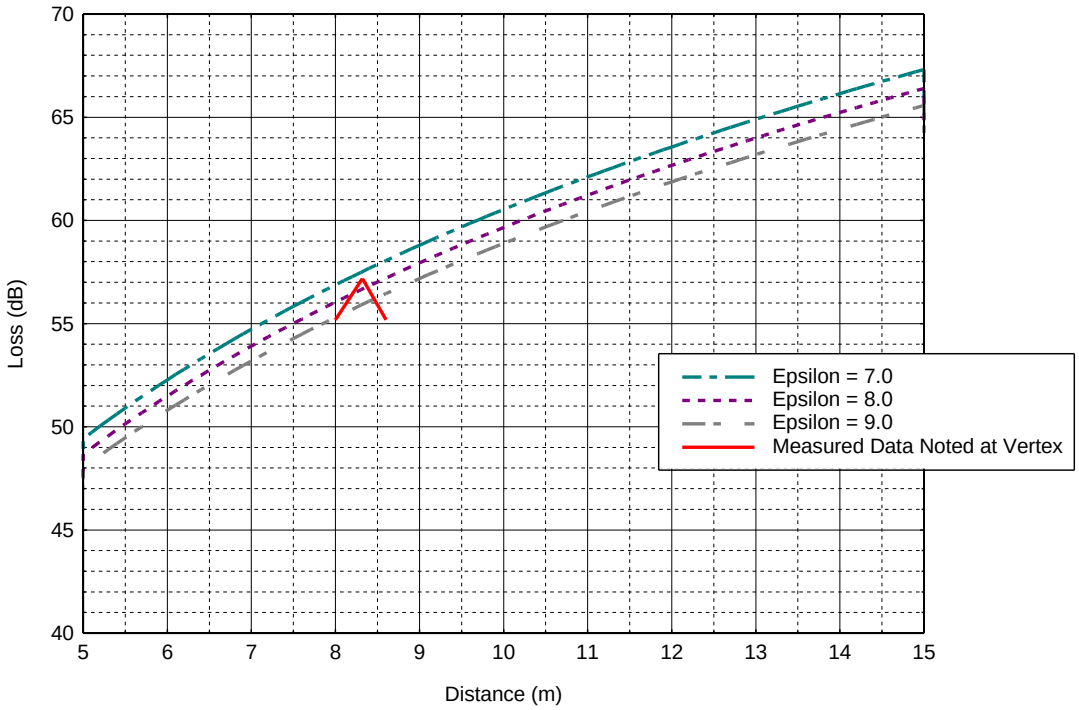

Figure A-22. Comparisons of propagation loss predictions with monopole measurements (May 2010) at 430 MHz with σ = 0.005.

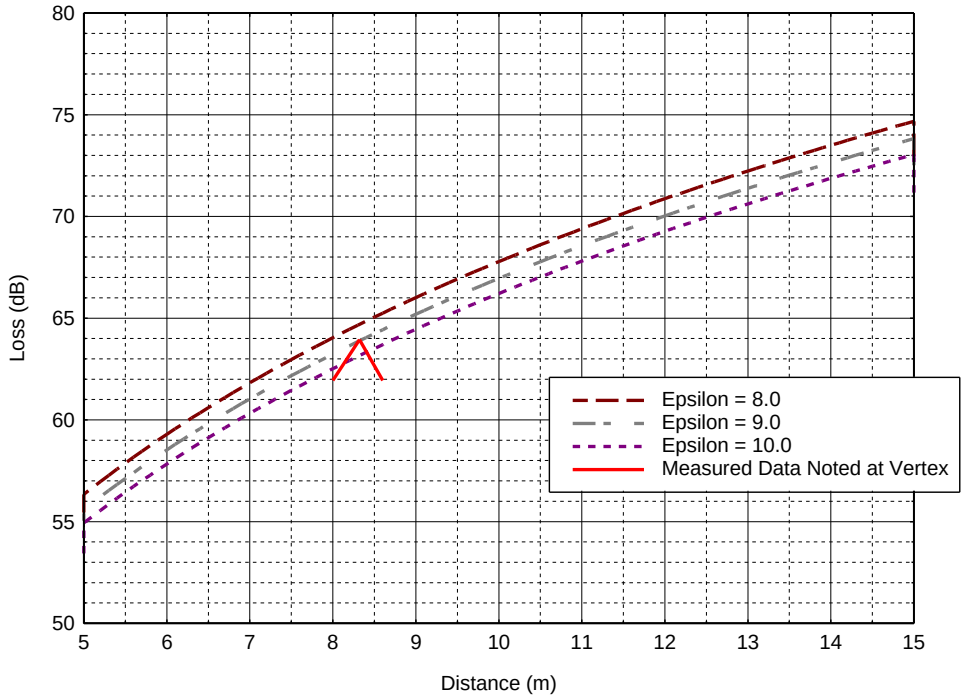

Figure A-23. Comparisons of propagation loss predictions with monopole measurements (May 2010) at 700 MHz with σ = 0.005.

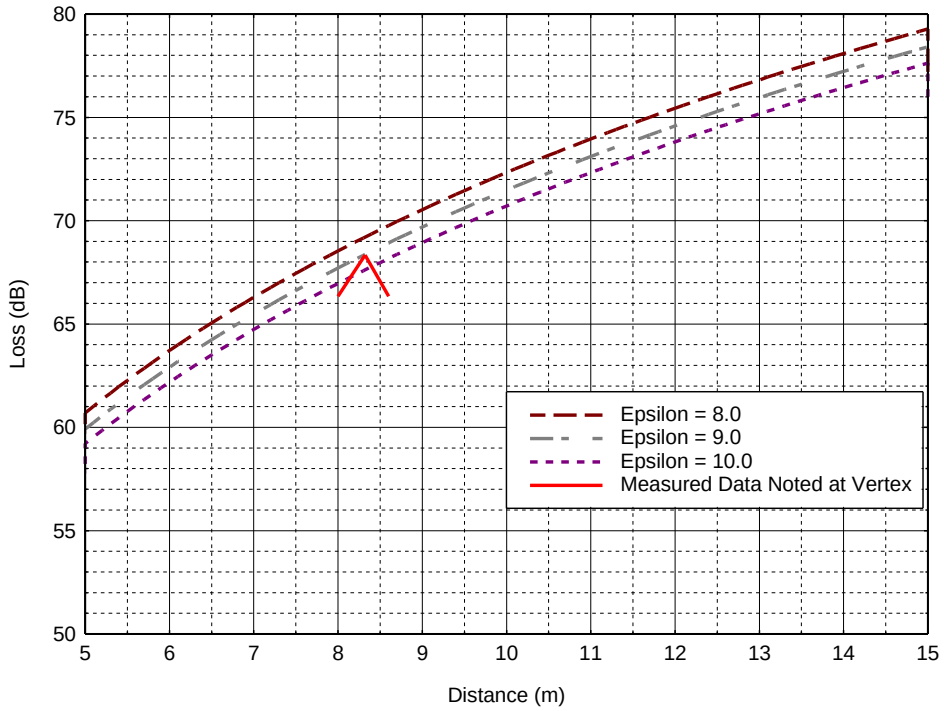

Figure A-24. Comparisons of propagation loss predictions with monopole measurements (May 2010) at 915 MHz with $\sigma = 0.005$.

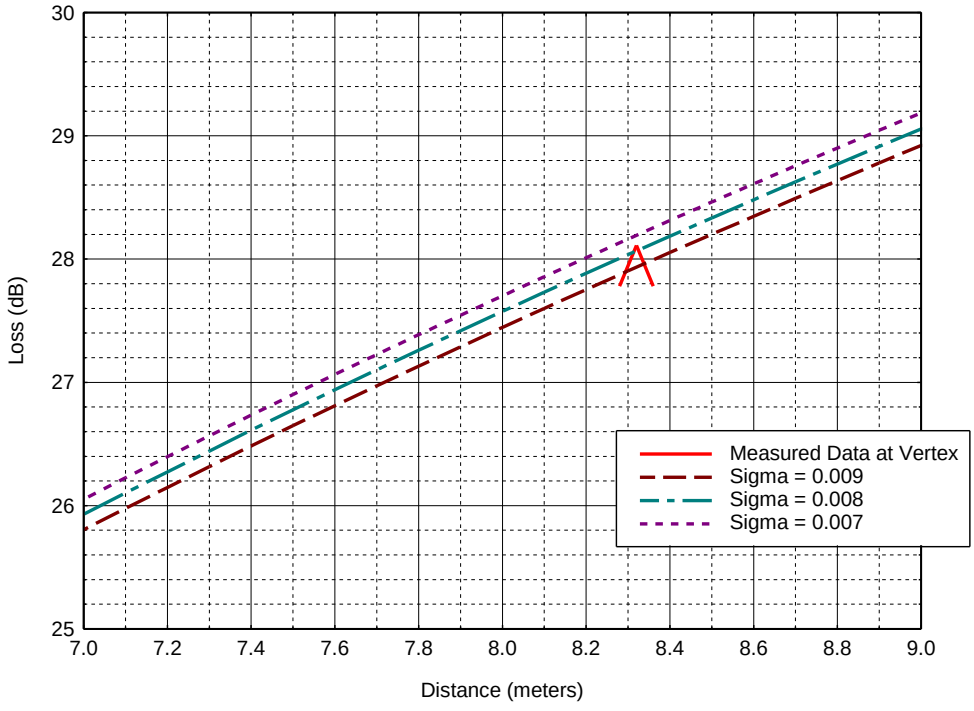

Figure A-25. Comparisons of propagation loss with monopole measurements (May 2010) at 60 MHz with varying σ and $\varepsilon_r = 7.0$.

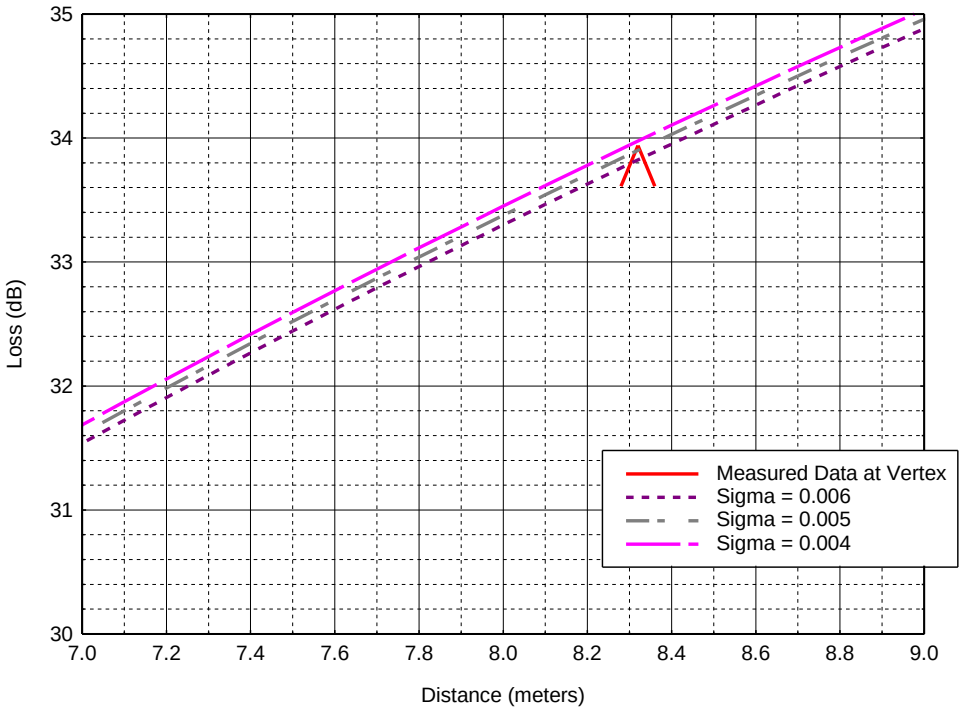

Figure A-26. Comparisons of propagation loss with monopole measurements (May 2010) at 90 MHz with varying σ and ε_r = 7.0.

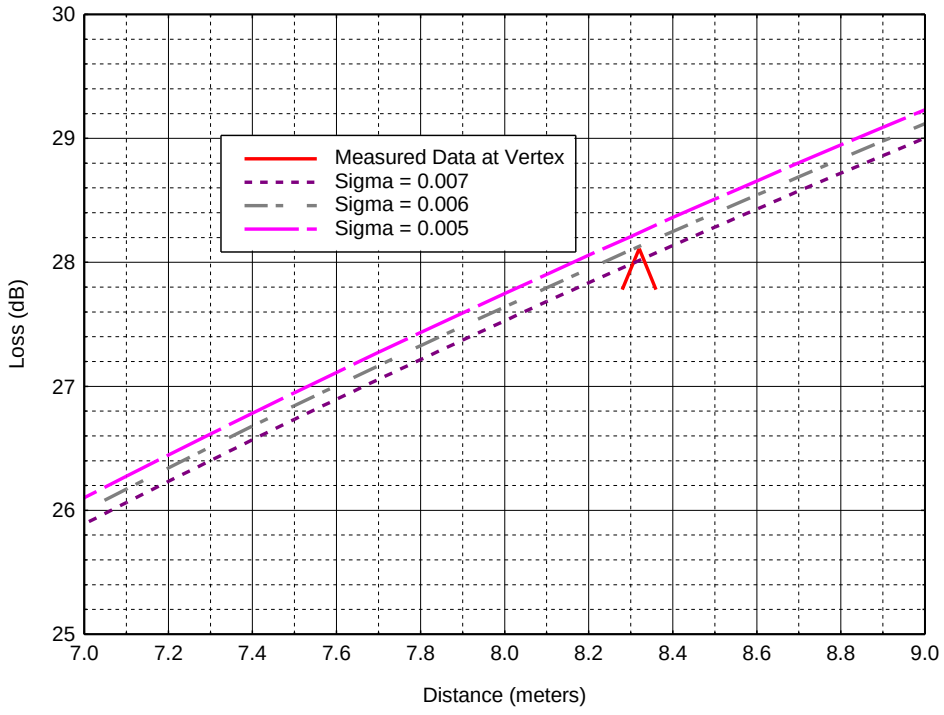

Figure A-27. Comparisons of propagation loss with monopole measurements (May 2010) at 60 MHz with varying σ and ε_r = 7.5.

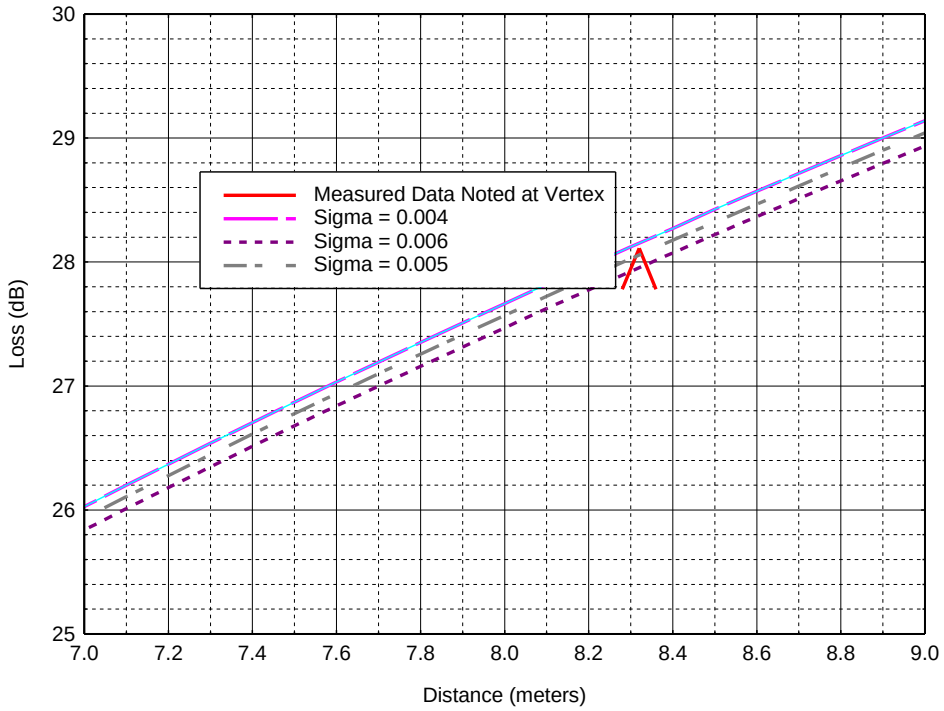

Figure A-28. Comparisons of propagation loss with monopole measurements (May 2010) at 60 MHz with varying σ and ε_r = 8.0.

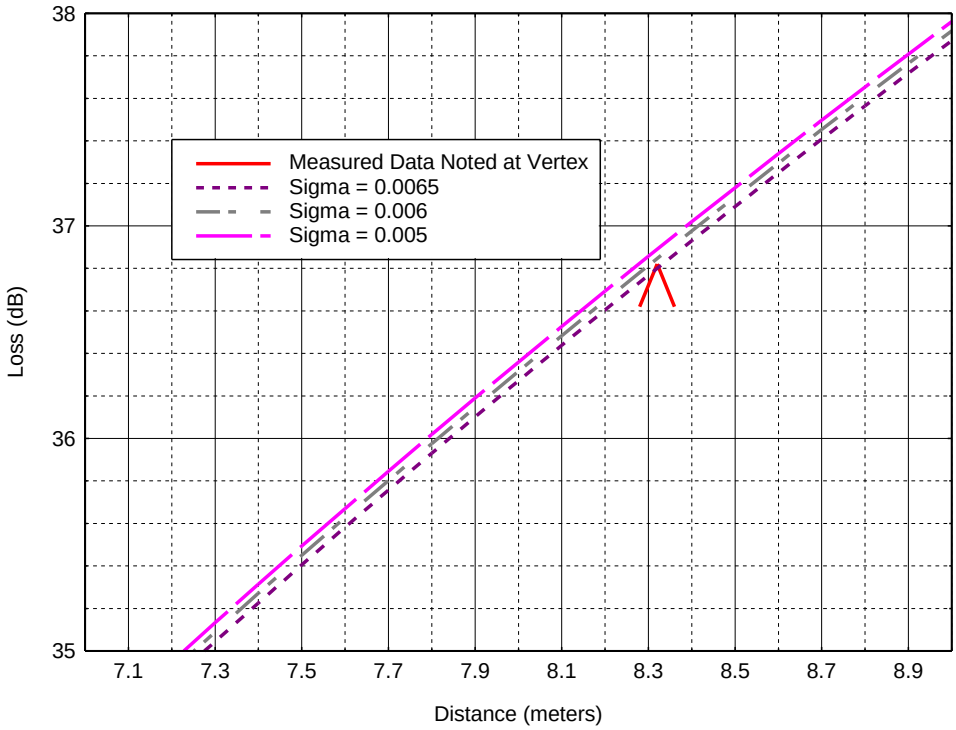

Figure A-29. Comparisons of propagation loss with monopole measurements (May 2010) at 120 MHz with varying σ and ε_r = 9.0.

FORM **NTIA-29** (4-80)

U.S. DEPARTMENT OF COMMERCE
NAT'L. TELECOMMUNICATIONS AND INFORMATION ADMINISTRATION

BIBLIOGRAPHIC DATA SHEET

1. PUBLICATION NO.	2. Government Accession No.	3. Recipient's Accession No.
TR-12-484		

4. TITLE AND SUBTITLE	5. Publication Date
Free-Field Measurements of the Electrical Properties of Soil Using the Surface Wave Propagation Between Two Monopole Antennas	January 2012
	6. Performing Organization Code: NTIA/ITS.E

7. AUTHOR(S)	9. Project/Task/Work Unit No.
Nicholas DeMinco, Robert T. Johnk, Paul McKenna, Chriss A. Hammerschmidt, J. Wayde Allen	3141000-300

8. PERFORMING ORGANIZATION NAME AND ADDRESS	10. Contract/Grant Number.
Institute for Telecommunication Sciences National Telecommunications & Information Administration U.S. Department of Commerce 325 Broadway Boulder, CO 80305	

11. Sponsoring Organization Name and Address	12. Type of Report and Period Covered
National Telecommunications & Information Administration Herbert C. Hoover Building 14th & Constitution Ave., NW Washington, DC 20230	

14. SUPPLEMENTARY NOTES

15. ABSTRACT (A 200-word or less factual summary of most significant information. If document includes a significant bibliography or literature survey, mention it here.)

This report describes one of three free-field, radio-frequency (RF) measurement systems that are currently being developed by engineers at the Institute for Telecommunication Sciences (NTIA/ITS).The objective is to provide estimates of the electrical properties of the ground (permittivity and conductivity) over which they are deployed. This measurement system uses transmission loss measurements between two monopoles placed close to the ground at specific separation distances. Soil properties are extracted by comparing measured data with known analytical models and optimizing the results.

16. Key Words (Alphabetical order, separated by semicolons)

17. AVAILABILITY STATEMENT	18. Security Class. (This report)	20. Number of pages
☒ UNLIMITED.	Unclassified	51
☐ FOR OFFICIAL DISTRIBUTION.	19. Security Class. (This page)	21. Price:
	Unclassified	

NTIA FORMAL PUBLICATION SERIES

NTIA MONOGRAPH (MG)

A scholarly, professionally oriented publication dealing with state-of-the-art research or an authoritative treatment of a broad area. Expected to have long-lasting value.

NTIA SPECIAL PUBLICATION (SP)

Conference proceedings, bibliographies, selected speeches, course and instructional materials, directories, and major studies mandated by Congress.

NTIA REPORT (TR)

Important contributions to existing knowledge of less breadth than a monograph, such as results of completed projects and major activities. Subsets of this series include:

NTIA RESTRICTED REPORT (RR)

Contributions that are limited in distribution because of national security classification or Departmental constraints.

NTIA CONTRACTOR REPORT (CR)

Information generated under an NTIA contract or grant, written by the contractor, and considered an important contribution to existing knowledge.

JOINT NTIA/OTHER-AGENCY REPORT (JR)

This report receives both local NTIA and other agency review. Both agencies' logos and report series numbering appear on the cover.

NTIA SOFTWARE & DATA PRODUCTS (SD)

Software such as programs, test data, and sound/video files. This series can be used to transfer technology to U.S. industry.

NTIA HANDBOOK (HB)

Information pertaining to technical procedures, reference and data guides, and formal user's manuals that are expected to be pertinent for a long time.

NTIA TECHNICAL MEMORANDUM (TM)

Technical information typically of less breadth than an NTIA Report. The series includes data, preliminary project results, and information for a specific, limited audience.

For information about NTIA publications, contact the NTIA/ITS Technical Publications Office at 325 Broadway, Boulder, CO, 80305 Tel. (303) 497-3572 or e-mail info@its.bldrdoc.gov.

This report is for sale by the National Technical Information Service, 5285 Port Royal Road, Springfield, VA 22161,Tel. (800) 553-6847.